COMMUNICATIONS IN COMPUTATIONAL PHYSICS
Vol. **1**, No. 2, pp. 228-258

Commun. Comput. Phys.
April 2006

FIFA — Fast Interpolation and Filtering Algorithm for Calculating Dyadic Green's Function in the Electromagnetic Scattering of Multi-Layered Structures

Tiejun Yu*[1] and Wei Cai[2]

[1] *Sigrity Inc., 4675 Stevens Creek Blvd, Santa Clara, CA 95051, USA.*
[2] *Department of Mathematics, University of North Carolina at Charlotte, Charlotte, NC 28223, USA.*

Received 8 September 2005; Accepted (in revised version) 10 November 2005

Abstract. The dyadic Green's function in multi-layer structures for Maxwell equations is a key component for integral equation method, but time consuming to calculate. A novel algorithm Fast Interpolation and Filtering Algorithm (FIFA) for the calculation of the dyadic Green's function in multi-layer structures is proposed in this paper. We discuss in specific details, ready for use in practical calculations of scattering in layer media, how to apply FIFA to calculate various components of the dyadic Green's function. The algorithm is based on two techniques: interpolation of Green's function both in the spectral domain and spatial domain and low pass filter window based acceleration. Compared to the popular Complex Image Method (CIM), FIFA provides the same speed and overcomes several difficulties associated with CIM while being more general and robust. Specifically, there are no limitation on the frequency range, the number of layers in the structure and the type of Green's functions to be calculated, and moreover, no need to extract surface wave poles from the spectral form of the Green's function. Numerical results are given to demonstrate the efficiency and robustness of the proposed method.

Key words: Fast interpolation and filtering algorithm (FIFA); complex image method (CIM); low pass filter window (LPFW); interpolation table (IT); electromagnetic (EM).

1 Introduction

A typical numerical method for electromagnetic (EM) scattering [4,5,14] and parameter extraction of VLSI, IC and their packaging [2,6,7,16] is the integral equation (IE) based method of moments (MoM) [15]. Discretization using Rao-Wilton-Glission basis functions (RWG) [3] is

*Correspondence to: Tiejun Yu, Sigrity Inc., 4675 Stevens Creek Blvd, Santa Clara, CA 95051, USA. Email: tyu@sigrity.com

usually used for the surface IE. The main advantage of the integral formulation is its reduced number of unknowns and flexibility in handling complex geometry of the scatter surface and automatic enforcement of Sommerfeld exterior outgoing conditions via appropriate Green's function [11, 12]. Generally speaking, there are three steps in the computation of such a problem: matrix filling, matrix inversion, and calculation of scattering field and parameter extraction. For a large size problem, the calculation in the second step is dominant and extensive researches have been done in that regard [7, 19–23]. For a moderate size problem, the CPU time used in the first and the third steps, which include the calculation of dyadic Green's function, is much more than that needed for matrix inversions. Therefore, it is necessary to investigate fast evaluation methods for Green's function. In many cases, such as detection of buried targets, parameter extraction of VLSI and its packaging, numerical modeling of the printed structure used in the monolithic millimeter and microwave circuits (MMIC), the effect of the object's complicated environments can be simply represented by a multi-layered structure model which requires multi-layered Green's function. The spatial or time domain Green's function for a multi-layered medium can be expressed in the form of a Hankel transform of the spectral Green's function. Though the spectral Green's function can be derived explicitly [8, 11, 12], it is extremely time-consuming to get time domain Green's function. This is because the kernel of the Hankel transform contains a Bessel function that oscillates fast (especially when the transverse distance between the source point and observation points is large) and decays slowly. There is extensive research literature in the field of fast calculation of Green's function [9, 10], most of them are based on complex image method (CIM) using the Prony method and the well-known Sommerfeld identity (SI) [17]. CIM is an important useful technique for the Green's function calculation when the source and field points remain in the same layer and the frequency belongs to some limited range. However, in some cases, CIM seems not to work when there is difficulty in extracting the poles from the spectral form of Greens function and when the source and field points are located in different layers. In [4, 5], an efficient evaluation method of Green's function was proposed, based on the integration along a steepest-descent path (SDP) and leading-order approximations of such integrals. However, it is only valid for a simple structure, e.g. half space case, in which the SDP can be found. In this paper, we propose and study a robust and general method of fast Green's function calculation for multi-layered structures - Fast Interpolation and Filtering Algorithm (FIFA). As its name suggests, the method is based on interpolation of Green's function in spectral domain (SD) and time domain (TD), and acceleration by a low-passing filter window function.

The rest of the paper will be organized as follows. In Section 2 we present the specifications of Green's functions for layered structure, an appendix is introduced containing a complete listing of the spectral forms and time domain forms of the components in the dyadic Green's function. A less complete discussion of the spectral Green's function can be found in [11], to our knowledge, this is the first complete presentation of potential and electromagnetic field Green's function in both time and spectral domain. Researchers in scattering of multilayer structure should find it handy for implementation. We will discuss the Complex Image Method (CIM) and its difficulties in Section 3. Section 4 introduces the new method FIFA. Section 5 will contain some implementation issues of the FIFA while Section 6 presents numerical results of the FIFA

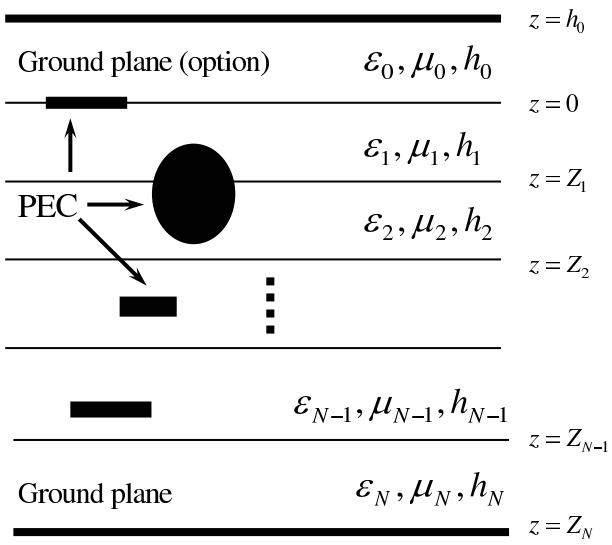

Figure 1: Mutli-layer structure with 3-D perfect electrical conducting (PEC) objects embedded in it.

for several practical microwave structures. Finally, a conclusion is given in Section 7.

2 Green's function in layered structure

2.1 Problem setup

Fig. 1 is a multi-layer structure of interest for this paper. There are two optional perfect electric conducting (PEC) ground planes at the bottom and top of the structure. Each layer is defined by its permittivity, permeability and thickness: $\varepsilon_{ri}\varepsilon_0$, μ_i, h_i, $i = 0, 1, \ldots, N$. Throughout the paper, the time dependence of $e^{j\omega t}$ is assumed and suppressed. Only the Green's function of the electric current source is considered here, while Green's function for magnetic current source can be derived by a dual procedure.

The electric field Green's function is defined by

$$\nabla \times \nabla \times \overline{G}_E^{ji} - k_j^2 \overline{G}_E^{ji} = -j\omega\mu_i \bar{I}\delta(r - r'), \quad j = \sqrt{-1}, \tag{2.1}$$

and the electric field can be expressed as

$$E^j(r) = \int \overline{G}_E^{ji}(r/r') \cdot J(r')dr' \tag{2.2}$$

where $\overline{G}_E^{ji}$ is the electric field dyadic Green's function that represents the electric field in the j^{th} layer due to the unit-strength, arbitrary oriented current dipole in the i^{th} layer. From the Maxwell equations, the magnetic field dyadic Green function can be written as

$$\overline{G}_H^{ji}(r, r') = -\frac{1}{j\omega\mu} \nabla \times \overline{G}_E^{ji}(r, r'), \tag{2.3}$$

and the magnetic field can be expressed as

$$H^j(r) = \int \overline{G}_H^{ji}(r/r') \cdot J(r')dr'. \tag{2.4}$$

Usually, a mixed-potential integral equation (MPIE) is preferred, and the fields are then represented by potentials:

$$E^j(r) = -j\omega A^j(r) - \nabla\phi^j(r) \tag{2.5}$$

$$H^j(r) = \frac{1}{\mu_j}\nabla \times A^j(r). \tag{2.6}$$

Therefore, potential Green's functions are needed to represent the potentials as following:

$$A^j(r) = \int \overline{G}_A^{ji}(r/r') \cdot J(r')dr' \tag{2.7}$$

$$\phi^j(r) = \int G_V^{ji}(r/r')q(r')dr' \tag{2.8}$$

where A^j is the magnetic vector potential in the j^{th} layer due to the current density $\mathbf{J}$ in the i^{th} layer, ϕ^j is the corresponding scalar potential related to A^j through the Lorenz gauge condition. $\overline{G}_A^{ji}$ is the dyadic Green's function which represents the magnetic vector potential in the j^{th} layer due to the unit-strength, arbitrary oriented current dipole in the i^{th} layer. G_V^{ji} is Green's function which represents the scalar potential in the j^{th} layer due to the charge associated with unit-strength, arbitrary oriented current dipole in the i^{th} layer. Choosing the formulation C proposed in [11], $\overline{G}_A^{ji}$ is modified and can be expressed in form of

$$\overline{G}_A^{ji} = (\hat{x}\hat{x} + \hat{y}\hat{y})\overline{G}_A^{xx,ji} + \hat{z}\hat{z}\overline{G}_A^{zz,ji} + \hat{x}\hat{z}\overline{G}_A^{xz,ji} + \hat{y}\hat{z}\overline{G}_A^{yz,ji} + \hat{z}\hat{x}\overline{G}_A^{zx,ji} + \hat{z}\hat{y}\overline{G}_A^{zy,ji} \tag{2.9}$$

or in the matrix form

$$\overline{G}_A^{ji} = \begin{bmatrix} G_A^{xx,ji} & 0 & G_A^{xz,ji} \\ 0 & G_A^{xx,ji} & G_A^{yz,ji} \\ G_A^{zx,ji} & G_A^{zy,ji} & G_A^{zz,ji} \end{bmatrix}. \tag{2.10}$$

In this case, G_V^{ji} represents the scalar potential in the j^{th} layer due to the charge associated with unit-strength, horizontal oriented current dipole in the i^{th} layer.

In general, $\overline{G}_E^{ji}, \overline{G}_H^{ji}$ have higher singularity compared to $\overline{G}_A^{ji}, G_V^{ji}$, as a result, the electrical field IE (EFIE) whose integral kernel includes $\overline{G}_E^{ji}$ is less attractive than the MPIE formulation whose integral kernel includes $\overline{G}_A^{ji}$ and G_V^{ji}.

2.2 Green's function in spectral domain

Using equivalent network techniques [8, 11], the multi-layered dyadic Green's functions in the spectral domain (SD) can be expressed in terms of the following k_p-dependent functions summarized in Table 1 (see the Appendix for details).

Table 1: Green's Function in Spectral Domain

$\widetilde{G}$	$\widetilde{G}_{eyx}$	$\widetilde{G}_1$	$\widetilde{G}_{hxz}$	$\widetilde{G}_{azx}$	$\widetilde{G}_5$	$\widetilde{G}_{exxm}$	$\widetilde{G}_{eyxw}$	$\widetilde{G}_{exz}$	$\widetilde{G}_3$	$\widetilde{G}_{kxy}$	$\widetilde{G}_{1z}$	$\widetilde{G}_h$	$\widetilde{G}_{azx\rho}$	$\widetilde{G}_{eyxz}$
I-SD	0	1	2	3	6	5	9	8	7	4	10	11	12	13

Table 2: Relationship between Green's function in time and spectral domain.

I-TD	*I-SD*	G	*Relationship*
0	0	g_v	$g_v = S_0[\widetilde{G}_{eyx}]$
1	1	g_{axx}	$g_{axx} = S_0[\widetilde{G}_1]$
2	2	g_{azz}	$g_{azz} = S_0[\widetilde{G}_{hxz}]$
3	3	$g_{az\rho}$	$g_{az\rho} = S_1[\widetilde{G}_{azx}]$
4	4	$g_{a\rho z}$	$g_{a\rho z} = S_1[\widetilde{G}_{kxy}]$
5	5	g_{exx2}	$g_{exx2} = S_0[\widetilde{G}_{exxm}]$
6	6	g_{ezz}	$g_{ezz} = S_0[\widetilde{G}_5]$
7	7	$g_{ez\rho}$	$g_{ez\rho} = S_1[\widetilde{G}_3]$
8	8	$g_{e\rho z}$	$g_{e\rho z} = S_1[\widetilde{G}_{exz}]$
9	9	g_{exx1}	$g_{exx1} = S_2[\widetilde{G}_{eyxw}]$
10	12	$g_{h\rho}$	$g_{h\rho} = S_0[\widetilde{G}_{azx\rho}]$
11	10	g_{h1z}	$g_{h1z} = S_0[\widetilde{G}_{1z}]$
12	1	$g_{hz\rho}$	$g_{hz\rho} = S_1[\widetilde{G}_1]$
13	11	$g_{h\rho z}$	$g_{h\rho z} = S_1[\widetilde{G}_h]$
14	3	g_{hxx}	$g_{hxx} = S_2[\widetilde{G}_{azx}]$
15	0	$g_{v\rho}$	$g_{v\rho} = S_1[\widetilde{G}_{eyx}]$
16	13	g_{vz}	$g_{vz} = S_0[\widetilde{G}_{eyxz}]$

In Table 1, *I-SD*, the identifier of the Green's function in spectral domain, is assigned to each spectrum form for the convenience of bookkeeping. All of those spectral functions in the Table 1 are arranged according to the characteristics of radical symmetry. Field and source layer indices j, i are suppressed for simpler notation. The relations between these spectra and $\overline{\widetilde{G}}_E$, $\overline{\widetilde{G}}_H$, $\overline{\widetilde{G}}_A$, $\overline{\widetilde{G}}_V$ are given in the Appendix.

2.3 Green's function in spatial domain (or time domain)

In this paper, we will use term "spatial domain" or "time domain" Green's function without distinction to indicate $G(\rho, z; z') = G(x, y, z; z')$. Using 2D Fourier Transform, which can be changed into a Sommerfeld integration (see Appendix), Green's function in the time domain (TD) or spatial domain can be obtained and summarized in Table 2.

In Table 2, *I-TD*, the time domain (TD) identifier of the Green's function, is assigned to the each time domain Green's function. All the time domain Green's functions in the Table 2 are

also arranged according to the characteristics of radical symmetries, and to the type of spectral form Green's functions $\overline{G}_E^{ji}$, $\overline{G}_H^{ji}$, $\overline{G}_A^{ji}$, $\overline{G}_V^{ji}$, can be expressed with.

3 Complex image method

Sommerfeld integration defined in Table 2 is needed to obtain Green's functions in time domain. Complex image method (CIM) is a popular technique in the electrical engineering community for this purpose. In the following, the closed-form of Green's function using complex image method (CIM) and its drawbacks are discussed. CIM is based on the well known Sommerfeld identity [17]:

$$\frac{e^{-jkr}}{r} = \frac{1}{2j}\int_{SIP} dk_\rho k_\rho H_0^{(2)}(k_\rho\rho)\frac{e^{-jk_z|z|}}{k_z} = -j\int_{sip} dk_\rho k_\rho J_0(k_\rho\rho)\frac{e^{-jk_z|z|}}{k_z} \tag{3.1}$$

where H_0^2 is the Hankel function of the second kind and SIP is the Sommerfeld integration path integration path $(-\infty,\infty)$. J_0 is the first order *Bessel* function and *sip* is the Sommerfeld integration path $(0,\infty)$. To use (3.1) and eliminate the need for numerical integrations in Table 2, the spectral-domain Green's function is approximated by a series of complex exponentials, which is obtained by Prony method or the generalized pencil of function method (GPOF) [18] using one step [10], two-step [9] or three-step approach [18] along the integration path shown in the Fig. 2 denoted by $P2$. As a result, the spectral-domain Green's functions are represented in the form

$$\widetilde{G} \approx \frac{1}{j2k_z}\left(\sum_{n=1}^{N_1} a_{1n}e^{-jb_{1n}k_{zi}} + \sum_{n=1}^{N_2} a_{2n}e^{-jb_{2n}k_{zi}} + \cdots\right) \tag{3.2}$$

Thus, using (3.1), Green's function in the time domain can be approximated as

$$G \approx \sum_{n=1}^{N_1} a_{1n}\frac{e^{-jk_i r_{1n}}}{r_{1n}} + \sum_{n=1}^{N_2} a_{2n}\frac{e^{-jk_i r_{2n}}}{r_{2n}} + \cdots \tag{3.3}$$

where $r_{in} = \sqrt{\rho^2 - b_{in}^2}$, $(i = 1, 2, \dots)$ and $\rho = \sqrt{x^2 + y^2}$, $k_i = \sqrt{k_\rho^2 + k_{zi}^2}$. The physical meaning of closed form (3.3) is that the effect of the layered structure can be replaced by a homogeneous background medium with a set of image sources with an amplitude of a_{in} located at a complex position r_{in}. Though CIM has been extensively studied and widely used for the printed and other simple layered structures, it has several serious drawbacks or limitations as follows. There is a strong need for a new robust way to overcome those difficulties and calculate the Green's functions accurately and efficiently.

3.1 Difficulty with high frequencies

For the Green's function in the spectral domain of multi-layered structures $\widetilde{G}$ includes many functions containing terms like $\coth(\sqrt{k^2 - k_\rho^2}h)$ which come from the transmitted impedances.

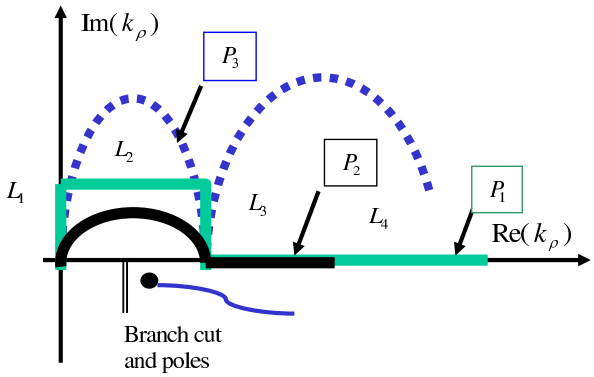

Figure 2: Sommerfeld Integral Path (SIP).

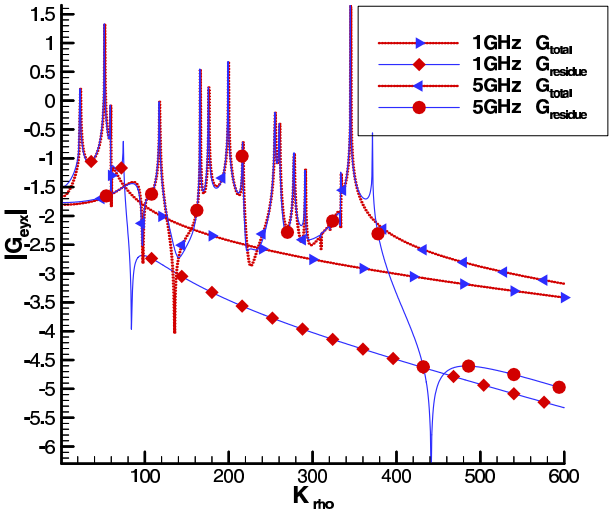

Figure 3: The comparison of Green's function in spectral domain. Here G_{total} means the spectral without extracting the direct term, while $G_{residue}$ is the spectral after subtraction of the direct term. The multi-layer media has 6 layers with the top open and bottom closed by a PEC ground plane. $z = -0.0325$, $z' = -0.03$, the layer parameters are: the first layer is the air layer, the others are defined by: $\varepsilon_{r2} \cdots \varepsilon_{r6} = 4.0, 3.4, 12.56, 7.6, 9.6$. $h_2, h_3, \cdots h_6 = 0.01, 0.01, 0.015, 0.015, 0.025$.

As the frequency is increased, $\widetilde{G}$ will oscillate fast on the L_2 section of the *sip* shown in the Fig. 2. Therefore, it would be difficult to account for the fast changes in the spectral domain without using tens of complex exponentials if not hundreds in certain cases. Fig. 3 shows the highly oscillatory nature of $\widetilde{G}$ for high frequencies. One can see that as the frequency increases from *1GHz (GigaHertz)* to *5GHz*, Green's function in the spectral domain becomes highly oscillatory. At higher frequency, without hundreds or even thousands terms of exponentials, it is impossible

to cast a function shown in Fig. 3 into the form of (3.2).

3.2 Difficulty with pole extractions

For the multi-layered structures, as the layer number increases, it is difficult to locate and extract the pole locations as usually required before using the Prony method or GPOF to cast the Green's function in spectral domain into a series of exponentials. One can use a two-level technique as described in [9] without pole extraction, but for a "bad-behavior" spectral-domain Green's functions of the multi-layered structure, hundreds (sometimes thousands) samples are needed in order to approximate the spectral Green's functions by exponential series, which results in inefficiency of the CIM.

3.3 Difficulty with multiple layers

Previous researches based on CIM using one-step [10], two-step [9] or three-step approach [18], focus only on the case in which the source and observation points are in the same layer. In the case when the source and field points are located in different layers, the spectral domain Green's function includes a mixed-factor which contains both the source and field layers wave number k_{zi}, k_{zj}. Using the half space case as an example,

$$\widetilde{G}_{eyx}^{01} = -\frac{2\varepsilon_{r1}e^{jk_{z1}z'-jk_{z0}z}}{k_{z0}\varepsilon_{r1}+k_{z1}}$$

has a mixed factor $(e^{jk_{z1}z'-jk_{z0}z})/(k_{z0}\varepsilon_{r1}+k_{z1})$, while $\widetilde{G}_{eyx}^{11}$ has a simple factor $(e^{jk_{z1}|z\pm z'|})/(k_{z1})$ only. Physically, it will be difficult (if not impossible) to cast a term including a mixed-factor into a series of simple factors without using other layer wave number information. Thus, using Prony method or GPOE to cast $\widetilde{G}$ into the form of (3.2) will lead to hundreds of terms in (3.3).

3.4 Difficulty with some types of G

CIM is based on the Sommerfeld identity (3.1), so only calculation of those Green's functions expressed in terms of $G = S_0[\widetilde{G}]$ can be possibly accelerated by CIM. Checking Table 2, only those Green's functions with *I-TD* $\in \{0, 1, 2, 5,\ 6, 10, 11, 16\}$ belong to this scenario. Other Green's functions are expressed in terms of $G = S_i[\widetilde{G}]$, $i = 1, 2$. Therefore, even after casting $\widetilde{G}$ into the form of (3.2), the Sommerfeld identity (3.1) can not be applied directly. Green's functions with *I-TD* $\in \{3, 4, 7, 8, 9,\ 12, 13, 14, 15\}$ belong to this case.

There is an alternative way to calculate those Green's function G with *I-TD* $\in \{3, 4, 7, 8, 9, 12, 13, 14, 15\}$ by CIM, but it will increase the computing complexity. The method is done in two steps: First force $\widetilde{G}$ into the form of (3.2), use the Sommerfeld identity (3.1) to obtain G in the form of (3.3). Second, take the operation of $\partial G/\partial x$, $\partial G/\partial y$ in the spatial domain if $G = S_1[\widetilde{G}]$, or take the operation of $\partial^2 G/\partial x^2$, $\partial^2 G/\partial y^2$, $\partial^2 G/\partial x \partial y$ in the spatial domain if $G = S_2[\widetilde{G}]$.

3.5 Difficulty with complex medium

For a lossy medium, the layer can be modeled with a complex relative dielectric constant $\varepsilon_{ri} = \varepsilon_r + \sigma/j\omega\varepsilon_0$, resulting in a complex value wave number $k_i^2 = \omega^2\varepsilon_i\mu = k_\rho^2 + k_{zi}^2$. The least square based Prony and the GPOF methods require uniform samplings along a real variable of a complex-valued function. If still sampled along the integral path by a 2-level CIM [9],

$$k_{zi} = \begin{cases} -jk_i[T_{02}+t] & 0 \le t \le T_{01} \text{ on path 2,} \\ k_i[-jt + (1 - t/T_{02})] & 0 \le t \le T_{02} \text{ on path 1,} \end{cases} \tag{3.4}$$

as k_i is a complex value, the integral variable k_ρ is traced on a path different from $P2$ but on a path shown as $P3$ in Fig. 2. In some cases, for example, when $f \to 0$, $\varepsilon_{ri} \to -j\infty$, the sampling path of k_ρ defined by (3.4) may be deformed dramatically which will lead to difficulty of casting the spectral domain Green's function into exponential series.

4 A general and robust method — FIFA

A new method — FIFA (Interpolation and Filtering Algorithm) - will use two ideas: Interpolation in spectral and time domains and acceleration by a low pass filter window, which will be discussed separately below.

4.1 Interpolation in spectral and time domains

As described above, CIM is a useful technique in many situations, but with many limitations. FIFA will include an interpolation idea based on the observation of the integrand for the n-th order Hankel transform

$$G(\rho) = S_n[\widetilde{G}(k_\rho)] = \int_0^\infty dk_\rho \widetilde{G}(k_\rho) J_n(k_\rho\rho) k_\rho^{n+1} \tag{4.1}$$

where G and $\widetilde{G}$ are the Green's functions in time domain (TD) and spectral domain(SD) listed in the Tables 1 and 2. $G \in G_{TD}$, $\widetilde{G} \in G_{SD}$, $n = 0, 1, 2$ and $G_{TD} = \{g_{h\rho}, g_{h1z}, g_{hz\rho}, g_{h\rho z}, g_{hxx}, g_{exx1}, g_{exx2}, g_{ez\rho}, g_{e\rho z}, g_{ezz}, g_{axx}, g_{azz}, g_{az\rho}, g_{a\rho z}, g_v, g_{v\rho}, g_{vz}\}$, $G_{SD} = \{\widetilde{G}_1, \widetilde{G}_3, \widetilde{G}_5, \widetilde{G}_h, \widetilde{G}_{1z}, \widetilde{G}_{eyx}, \widetilde{G}_{hxz}, \widetilde{G}_{azx}, \widetilde{G}_{kxy}, \widetilde{G}_{exz}, \widetilde{G}_{eyxw}, \widetilde{G}_{azx\rho}, \widetilde{G}_{eyxz}, \widetilde{G}_{exxm}\}$. We note that Green's function in spectral domain $\widetilde{G}$ in (4.1) is independent of ρ. For a given pair of (z, z'), we only need to calculate $\widetilde{G}(k_\rho, z/z')$ once and store it in an interpolation table labeled *G-SDIT*. Then for the hundreds or thousands of different ρ's need in the simulation, the interpolation table *G-SDIT* can be used repeatedly, resulting in a CPU time saving of 100's to 1000's times for the calculations of the spectral domain $\widetilde{G}(k_\rho, z/z')$. In practice, the interpolation table of $\widetilde{G}(k_\rho, z/z')$ is used for the *P1* in Fig. 2. The complex $\widetilde{G}$ depends on the distance that the sampling point travels along the integral path *P1* from the original point. The sampling density and interpolation table length will be determined by ρ_{max} and ρ_{min}, to be discussed in the following subsection. Compared to the complicated $\widetilde{G}(k_\rho, z/z')$, ρ dependence in $J_n(k_\rho\rho)$ is much simpler and can be calculated by simple approximation.

An interpolation strategy can also be designed for the time domain Green's function G_{TD}. As all elements in G_{SD} are arranged with the important characteristics of k_ρ dependence, the corresponding time domain Green's function G_{TD} are radical symmetric in ρ variable. Therefore, 4-D $(x-x', y-y', z, z')$ Green's function interpolation database for $G(r/r')$ can be reduced into a 3-D Green's function database $G(\rho, z/z')$. Further simplification can be done with respect to the discretization in the z direction. If the structure is discretized into N layers in z direction, the 3-D Green's function database $G(\rho, z/z')$ can be reduced to $N_{TDI} = N^2$ 1-D interpolation tabulations in spatial or time domain, *G-TDIT*. For a fixed pair of z/z', first calculate $\widetilde{G}(k_\rho, z/z')$ and generate the spectral domain interpolation table *G-SDIT*, then used the *G-SDIT* repeatedly and calculate all $G(\rho, z/z')$ for the different ρ in ρ_{min} to ρ_{max} and generate the time domain interpolation table *G-TDIT*. Then, repeat the same procedure for another pair of z/z' to establish all the time domain interpolation table *G-TDIT*. For some of the spectral domain Green's function G_{SD}'s (with *I-SD*$= 0, 1, 2$), they have reciprocity characteristics respect to z and z', the number of interpolation table for the time domain Green's functions can be further reduced to $N_{TDI} = (N+1)N/2$.

4.2 Acceleration by low pass filter window (LPFW)

The second feature of the FIFA is the use of an integration acceleration technique based on a low pass filter window (LPFW) in the spectral domain. As the integration length L_4 of sip in Fig. 2 is determined by ρ_{min}, L_4 may be still large when $z \to z'$. To reduce the length of integrating path L_4, a low-pass- filter- window (LPFW) function introduced in [27,28] is used to accelerate the calculation. The idea of the algorithm is to create an artificial steepest decent path by using a LPFW function ψ_a with a support size of a,

$$\psi_a(\rho) = \begin{cases} (1-(\rho/a)^2)^m & if\ \rho \le a, \\ 0 & otherwise. \end{cases} \tag{4.2}$$

Using the following identity for any cylindrical symmetrical function $f(\rho)$,

$$f(x,y) * \psi_a(x,y) = S_0[\widetilde{f}(k_\rho)\widetilde{\psi}(k_\rho)] \tag{4.3}$$

where $\rho^2 = x^2 + y^2$, $\widetilde{f}(k_\rho) = S_0[f(\rho)]$, $\widetilde{\psi}(k_\rho) = S_0[\psi(\rho)]$, $*$ denotes convolution.

To recover the value of $f(x,y)$ from the left-side of equation (4.3), using Taylor expansion for function $f(x,y)$ at the point (x,y) we obtain

$$f(x,y) * \psi_a(x,y) \approx M_0 f(x,y) + M_2(f_{xx}(\xi,0) + f_{yy}(\xi,0)) \tag{4.4}$$

where $0 \le \xi \le \rho$ and $M_0 = \pi a^2/(m+1)$, $M_2 = \int_{\rho \le a} \psi_a(x,y)x^2 dxdy$.

As a result of (4.3) and (4.4), $f(x,y)$ can be approximated as

$$f(x,y) = \frac{1}{M_0} S_o \left[\widetilde{f}(k_\rho)\widetilde{\psi}_a(k_\rho)\right](\rho) + \mathcal{O}(a^2) \quad \text{as } a \to 0. \tag{4.5}$$

Applying (4.5) to $G(\rho, z/z')$ leads to the following algorithm.

Algorithm 1: *Fast Algorithm for $G(\rho, z/z')$ when $\rho > a$*

$$G(\rho, z/z') = \frac{1}{M_0} W_0(\rho) + \mathcal{O}(a^2) \quad \text{as } a \to 0, \tag{4.6}$$

where

$$W_0(\rho) = S_0[\widetilde{G}(k_\rho, z/z')\widetilde{\psi}_a(k_\rho)]. \tag{4.7}$$

Remark 4.1. Algorithm 1 requires condition $\rho > a$ as the Green's function will not be smooth and the estimate in (4.4) will not hold.

Therefore, in order to apply the approximation (4.5) to function G for $\rho > a$, we will rewrite G as

$$G(\rho, z/z') = G_2(\rho, z/z')/r^2 \tag{4.8}$$

where $r = \sqrt{x^2 + y^2 + (z - z')^2} = \sqrt{\rho^2 + (z - z')^2}$. From the singularity property of the vector and scalar potential Green's function [33], $G_2(\rho, z/z') = r^2 G(\rho, z/z')$ is a smooth function, and the approximation (4.5) thus can be used for G_2. Meanwhile, we have the following identity [27]:

$$G_2(\rho, z/z') * \psi_a(x, y) = r^2 W_0(\rho) - 2\rho W_1(\rho) + W_2(\rho) \tag{4.9}$$

where W_0 is defined in (4.7) and

$$W_1(\rho) = S_1[\widetilde{G}(k_\rho, z/z')\widetilde{\psi}^*_a(k_\rho)/k_\rho] \tag{4.10}$$

$$W_2(\rho) = S_0[\widetilde{G}(k_\rho, z/z')\widetilde{\psi}^{**}_a(k_\rho)] \tag{4.11}$$

$$\widetilde{\psi}_a(k_\rho) = S_0[\psi_a(\rho)](k_\rho) = \int_0^a \psi_a(\rho) J_0(k_\rho \rho)\rho d\rho \tag{4.12}$$

$$\widetilde{\psi}^*_a(k_\rho) = S_1[\psi_a(\rho)](k_\rho) = \int_0^a \psi_a(\rho) J_1(k_\rho \rho)\rho^2 d\rho \tag{4.13}$$

$$\widetilde{\psi}^{**}_a(k_\rho) = S_0[\psi_a(\rho)\rho^2](k_\rho) = \int_0^a \psi_a(\rho) J_0(k_\rho \rho)\rho^3 d\rho. \tag{4.14}$$

Combining (4.4) and (4.9), a second approximation is obtained as follows.

Algorithm 2: *Fast Algorithm for $G(\rho, z/z')$ when $\rho \le a, a \to 0$*

$$G(\rho, z/z') = \frac{1}{r^2 M_0}\left[r^2 W_0(\rho) - 2\rho W_1(\rho) + W_2(\rho)\right] + \mathcal{O}(a^2). \tag{4.15}$$

In [28], the closed-forms of $\widetilde{\psi}_a$, $\widetilde{\psi}^*_a$, $\widetilde{\psi}^{**}_a$ were derived and the functions $\widetilde{\psi}_a$, $\widetilde{\psi}^*_a$, $\widetilde{\psi}^{**}_a$ were shown to have the following decaying properties when $|k_\rho| \to \infty$,

$$\left|\widetilde{\psi}_a(k_\rho)\right| = \mathcal{O}(|ak_\rho|^{-m}) \tag{4.16}$$

$$\left|\widetilde{\psi}^*_a(k_\rho)\right| = \mathcal{O}(|ak_\rho|^{-m+1}) \tag{4.17}$$

$$\left|\widetilde{\psi}^{**}_a(k_\rho)\right| = \mathcal{O}(|ak_\rho|^{-m}) \tag{4.18}$$

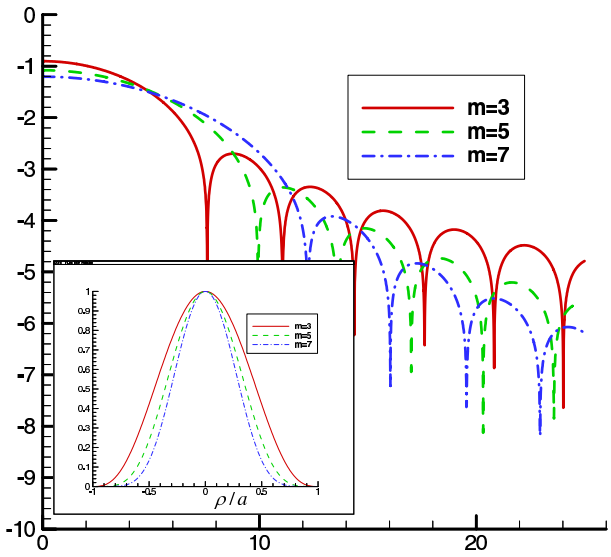

Figure 4: Window functions in both spectral and spatial domain. The larger figure is $\log(|\widetilde{\psi}_a(k_\rho)|)$, the insert $\psi_a(\rho)$. Here $a=1$, the order $m=3,5,7$.

where m is the order of the window function defined in (4.2). The fast decay condition of (4.16)-(4.18) insures that a short integration contour L_4 can be selected without sacrificing the accuracy of approximation of Algorithm 1 and 2. This means we have effectively created an artificial steep decent path for the Sommerfeld integration. Therefore, the size of the spectral Green's function interpolation table used in FIFA can be greatly reduced, and, the last segment L_4 will be determined by the decay properties of (4.16)-(4.18).

In practice, functions $\widetilde{\psi}_a$, $\widetilde{\psi}_a^*$ and $\widetilde{\psi}_a^{**}$ can be pre-calculated and stored in a separate interpolation table [28]. Fig. 4 shows both window functions ψ_a of order $m=3,5,7$ with support size $a=1$ (Lower left insert), and their frequency decays $\widetilde{\psi}_a$, respectively. Figs. 5 and 6 show the frequency decay of $\widetilde{\psi}_a^*$ and $\widetilde{\psi}_a^{**}$ with order $m=1,3,5,7$, support size $a=1$, respectively.

5 Implementation issues of FIFA

Integration Path: For each type of spectral Green's function $\widetilde{G}$ identified by *G-SDIT*, the integral path is simply chosen as *P1* shown in Fig. 2. *P1* is composed of 4 segments of length $L_i, i=1,2,3,4$, taken to have values

$$L_1 = L_3 = \beta k_0 \tag{5.1}$$

$$L_2 = \sqrt{\varepsilon_{r\max}+\alpha}k_0 \tag{5.2}$$

$$L_4 = \delta k_0 \tag{5.3}$$

where k_0 is the free space wave number, and α is a small positive number, such as 0.1. L_2 must cover all the poles and branch cut points. β is a small positive number, such as 0.005. By raising

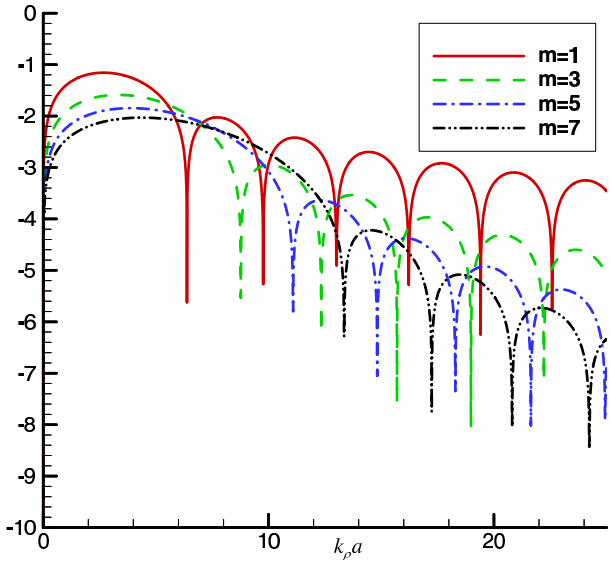

Figure 5: Window functions $\log(|\widetilde{\psi}_a^*(k_\rho)|)$, here $a = 1$, the order $m = 1, 3, 5, 7$.

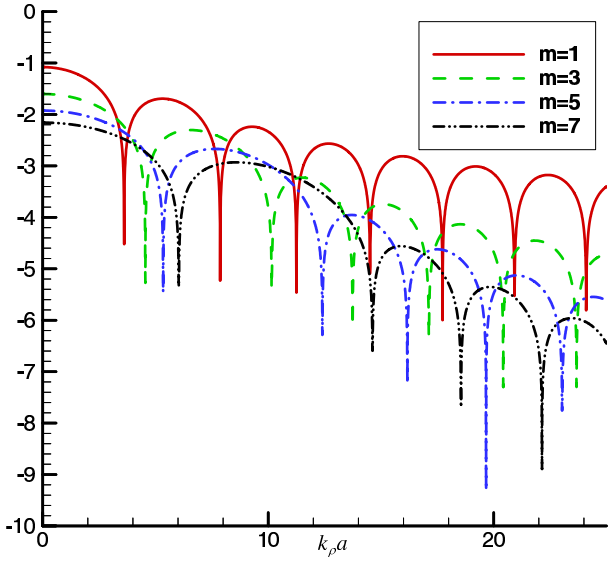

Figure 6: Window functions $\log(|\widetilde{\psi}_a^{**}(k_\rho)|)$, here $a = 1$, the order $m = 1, 3, 5, 7$.

the integral path L_2 by the height of L_1, we avoid all the poles and branch cut points. For larger L_1, $\widetilde{G}$ is smoother on L_2. However, if L_1 is too large, the accuracy of the approximation of $J_n(k_\rho\rho)$ will be comprised. Also, δ is a positive number which is decided adaptively by the value $\rho_{\min}$. For a fixed pair of z/z', when $\rho \in (\rho_{\min}, \rho_{\max})$ is changing, the convergence of $J_n(k_\rho\rho_{\min})$ is the slowest for all ρ, so when the *G-SDIT* is created, we just determine the L_4 adaptively

according to $1/\sqrt{k_\rho \rho_{\min}}$ until a convergence criterion is satisfied. Once L_4 is set by $\rho_{\min}$, for all other $\rho > \rho_{\min}$, the error of $G(\rho)$ will be better than the criterion error.

Sampling Density All the four segments are divided adaptively into a number of subintervals on which $\widetilde{G}$ are sampled to generate the interpolation table identified by *G-SDIT*. Different sampling strategies are used on the different segments. On the short segments L_1, L_3, uniform space sampling is used; On L_2, $\widetilde{G}$ varies fast, the density of sampling will be defined accordingly. As shown in Fig. 3, multi-layered spectral Green's function $\widetilde{G}$ oscillates faster at the end of L_2 due to the factors like $\coth(\sqrt{k^2 - k_\rho^2}h)$ in $\widetilde{G}$, so we proposed to divide segment L_2 into: $L_2 = l_1 + l_2 + \cdots + l_n$, and $l_i = (n - i + 1)l$, $l = 2L_2/(n^2 + n)$. On each sub-interval l_i we used same sampling points adaptively. On segment L_4, Green's function $\widetilde{G}$ is smooth, a sparse sampling can be used based mainly on the quasi-period of Bessel function $J_n(k_\rho \rho)$ function with an approximate periodicity $T \approx 2\pi/\rho$.

Also, we need to address the issue of singularities when the field point is approaching the source point in the calculation of Green's function. In the FIFA, when the source point and field point are located in different layers, there is no singularity problem. When the source and field points are located in the same layer, the Green's function in the Spectral domain can be decomposed into "direct" and "indirect" terms as defined in the appendix. The "direct" terms include the singularity feature and can be calculated by the Sommerfeld identity directly while the residual "indirect" terms can be obtained by FIFA.

Other implementation issues like high spectral approximation are also considered in FIFA. When the integral variable k_ρ is very large (compared to k_0), the integral kernel of Sommerfeld integration can be simplified by using the approximation of $\widetilde{G}$, for example, in the high spectral domain, we can use the fact that $\coth(\sqrt{k_\rho^2 - k_i^2}h_i) \approx 1$.

6 Numerical experiments and applications

A comprehensive code WDS (Wave Design Simulator) using FIFA has been developed to carry out 3-D full wave analysis of RF components and scattering of general objects in the arbitrary multi-layered media. Here, we first check the algorithm by calculate Green's function and compared with exact results, then we chose several application examples to demonstrate the efficiency and robustness of FIFA.

6.1 $\overline{G}_A(\rho, z/z'), G_v(\rho, z/z')$ of a five layered media

In this test case, the Green's functions $\overline{G}_A(\rho, z/z'), G_v(\rho, z/z')$ for a 5-layer media will be calculated by FIFA and compared to the direct Sommerfeld integration denoted as "exact" results. Four dielectric layers are used between the open air and a PEC ground plane. The relative dielectric constants for the four dielectric layers are, from top to bottom, 9.6, 12.5, 2.4, 3.6, respectively. The corresponding thicknesses are 1mm, 3mm, 2mm, 1.5mm, respectively.

Window ψ_a of order $m = 5$ with support size $a = 1$mm is used in FIFA and $L_4 = 20/a$ is used in the contour *P1* in Fig. 2. Fig. 8 contains the magnitude, imaginary and real part of the

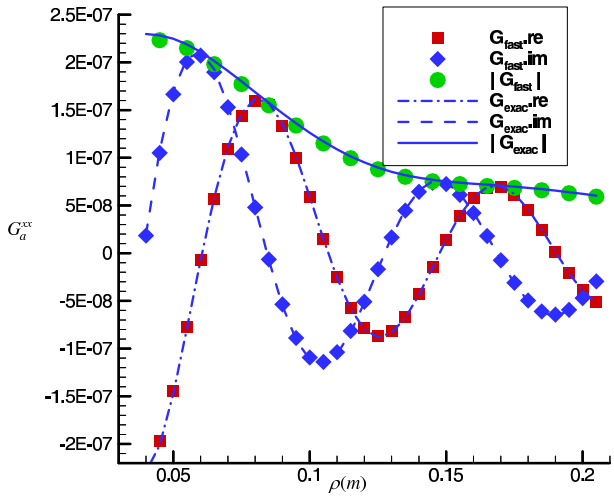

Figure 7: The comparison of $G_A^{xx}(\rho, z/z')$ for a 5-layered media. G_{fast} is obtained by FIFA and G_{exac} is calculated by direct Sommerfeld integration. L_4 used in the G_{exac} is 20 times longer than that used in G_{fast}. 100 sampling points are calculated in ρ direction, all G_{fast} at those points use the same *G-SDIT*, so FIFA is 2000 times fast than the direct Sommerfeld integration in this example.

scalar Green's function $G_v(\rho, z/z')$ with $z = -3.5$mm, $z' = -6.2$mm. Fig. 7 contains the Green's function $\overline{G}_A^{xx}(\rho, z/z')$ for the vector potential, again the magnitude, imaginary and real parts of this component are shown. The comparison between the results of FIFA and exact integration shows the high accuracy of FIFA.

6.2 Application in microstrip circuits

The first set of applications is from microstrip circuits, we use MPIE based MoM with hybrid RWG basis functions to obtain the S parameters [26] of the circuits. Our results denoted by "FIFA", the results by a commercial software Ansoft is denoted by "Ansoft". In these cases, the Green's function is relative simple and we used only two *G-TDIT* for each example, they are *G-TDIT* for $G_A^{xx,00}(\rho, 0/0)$ and $G_v^{00}(\rho, 0/0)$. For the Ansoft software, CIM is used to calculate Green's function. In these simple cases, our code is as fast as CIM. Fig. 9 shows a two-fan stub example. Fig. 10 is for the example of a band-pass filter, and Fig. 11 is for a low-pass filter. The geometry of the structures, the meshes, and the compared S parameters are included in the figures.

6.3 Application in parameter's extraction of VLSI and its package

To demonstrate the efficiency of FIFA, an example shown in the Fig. 12 is given and also compared with Ansoft software. It is a two layer structure with two ports, two strip lines connected with a cylindrical via. The Green's function used in this example is more complicated than that the case of microstrip circuits. If 4 Gaussian quadrature points are used for the

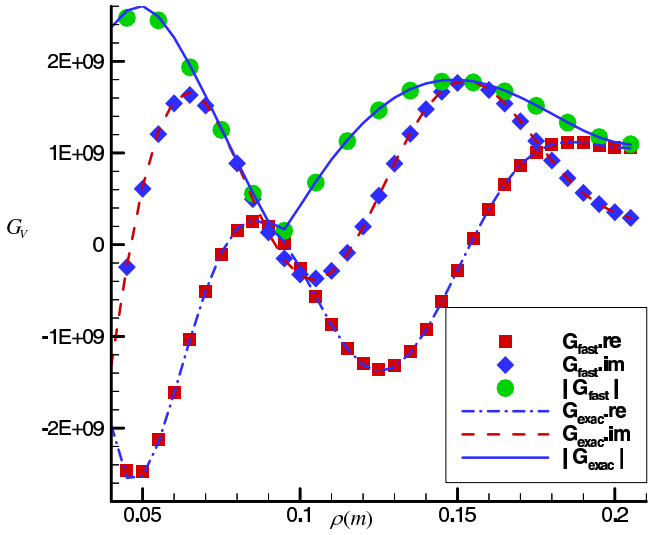

Figure 8: The comparison of $G_V(\rho, z/z')$ for a 5-layered media. G_{fast} is obtained by FIFA and G_{exac} is calculated by direct Sommerfeld integration. L_4 used in the G_{exac} is 20 times longer than that used in G_{fast}. 100 sampling points are calculated in ρ direction, all G_{fast} at those points use the same *G-SDIT*, so FIFA is 2000 times fast than the direct Sommerfeld integration in this example.

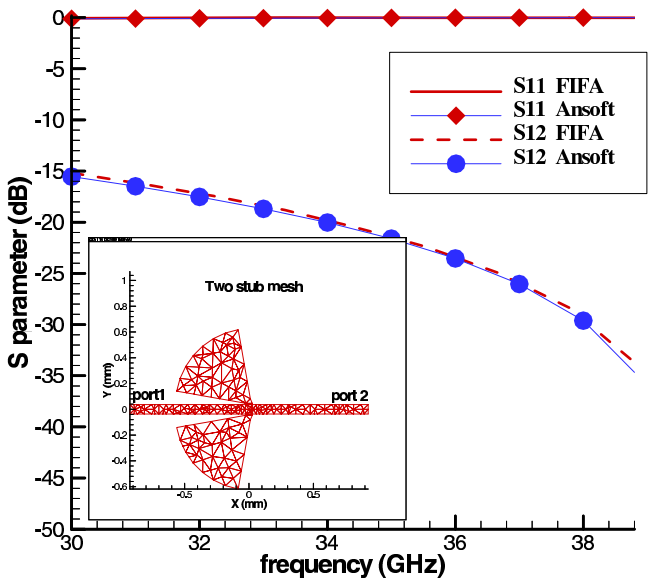

Figure 9: The comparison of S parameters of a two-stub fan printed circuit. The insert provides the geometry information and mesh discretization. The microstrip dielectric thickness is 0.1mm and $\varepsilon_r = 12.9$.

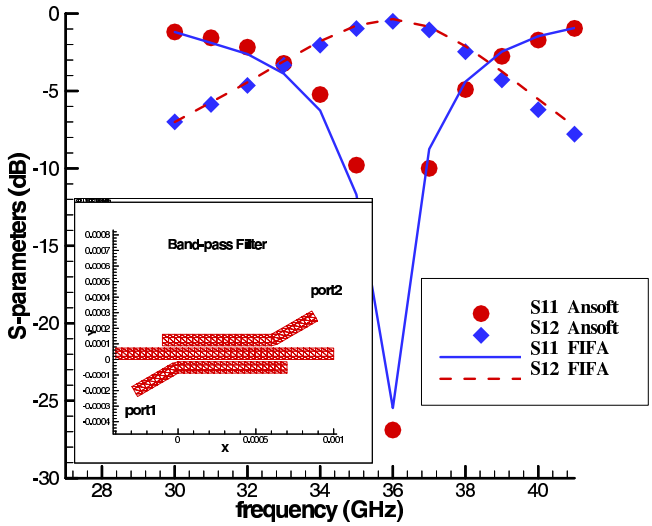

Figure 10: The comparison of S parameters of a microstrip band-pass filter. The insert provides the geometry information and mesh discretization. The microstrip dielectric thickness is 0.1mm and $\varepsilon_r = 12.9$.

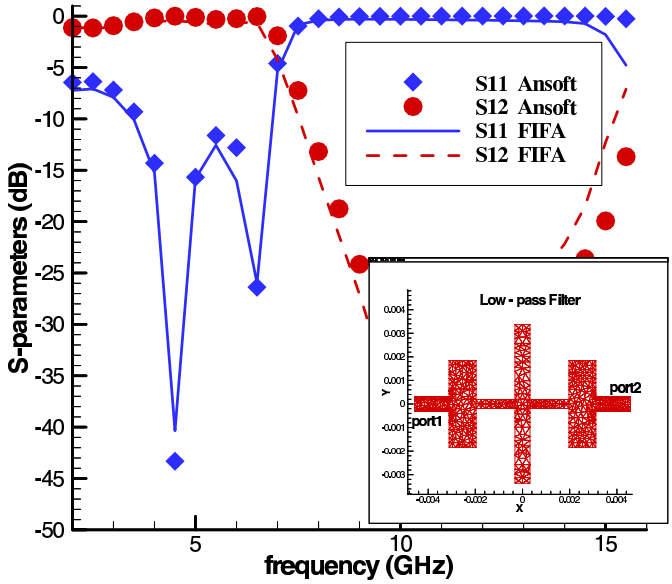

Figure 11: The comparison of S parameters of a microstrip low-pass filter. The insert provides the geometry information and mesh discretization. The microstrip dielectric thickness is 0.635mm and $\varepsilon_r = 9.6$.

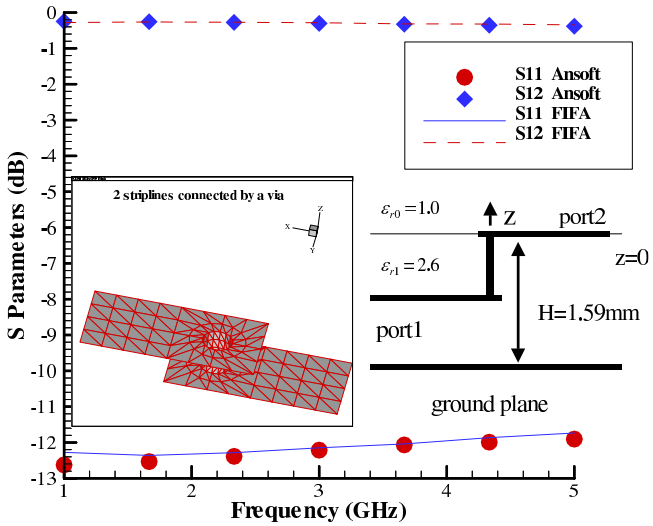

Figure 12: The comparison of S parameters of a structure composed by two strip lines connected by a via. The via is cylinder with diameter of 0.08485mm. Both of the strip lines width of 2.4mm and length of 4.8mm. Port1 is defined by two points (unit is mm): $(-3.6,-1.2,-0.795)$, $(-3.6,-1.2,-0.795)$. Port2 points are: $(3.6,-1.2,0)$, $(3.6,1.2,0)$. The insert is the mesh used.

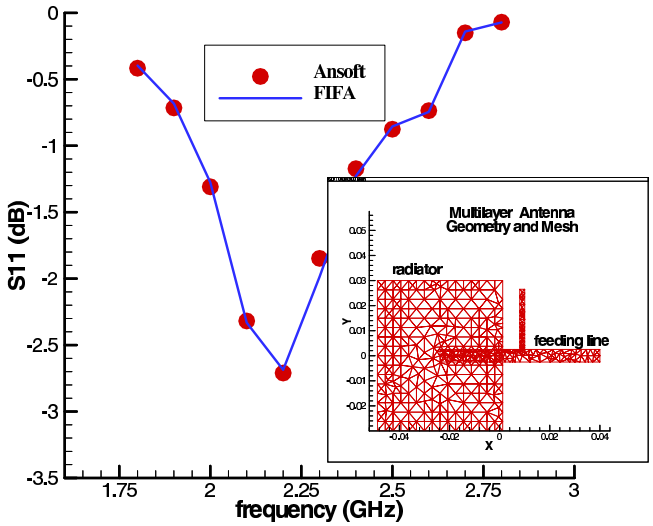

Figure 13: The comparison of S parameters of the multilayer antenna structure. It is a 3 layers structure. Layer 0 is the air layer with top open; Layer 1 and Layer 2 are dielectric layers with $h_1 = 1$mm, $h_2 = 4$mm, $\varepsilon_{r1} = 1.14$, $\varepsilon_{r2} = 1.12$. Layer 2 is closed by a PEC ground plane at bottom. Radiator is located at the air-dielectric interface and the feeding stripline is located on the interface of Layer 1 and Layer 2.

triangles on the via, the whole structure is discretized into 6 layers in z direction, the number of *G-TDIT* needed in the example is $N = 50$, where 21 tables for *G-TDIT* with *I-TD*= 0; 3 tables for *G-TDIT* with *I-TD*= 1; 8 for *G-TDIT* with *I-TD*= 3; 8 for *G-TDIT* with *I-TD*= 4; 10 for *G-TDIT* with *I-TD*= 2. Fig. 12 also shows the discretization of the structure. MPIE based MoM with RWG basis function is used to obtain the S parameters of the circuits, which is compared with the results calculated by the Ansoft software. Fig. 12 shows the compared results agree with each other very well. For this example, our code is about 10 times fast than Ansoft due to the speed of FIFA.

6.4 Application in multi-layer antenna

Fig. 13 shows a multi-layer wide-band antenna geometry structure and the compared S parameters (compared with Ansoft software). This is a three layers structure, the top layer is the air layer with top open; the middle layer with $h = 1$mm and $\varepsilon_{r1} = 1.14$; the bottom layer with $h = 4$mm and $\varepsilon_{r2} = 1.12$; the bottom is closed by a PEC ground plane. Radiating patch is located at the air-dielectric interface and the feeding strip-line is located on the interface between middle and bottom layers. The number of *G-TDIT* needed in the example is $N = 6$, where 3 for *G-TDIT* with *I-TD*= 0, 3 for *G-TDIT* with *I-TD*= 1.

7 Concluding remarks

A new method FIFA is proposed for the fast calculation of Green's function of multi-layered structures. The speed of the proposed algorithm results from two techniques: interpolation in spectral and time domain for the calculated Green's functions and integration acceleration by a low pass filter window. Compared to CIM, FIFA has the following properties and advantages:

1. It is a black-box approach good for any number of layers, and any types of Green's function;
2. It has no limitation on the frequency, the source types, the field and source point positions, the number of layers and the number of ground planes (0, 1 or 2 ground planes);
3. There is no need to extract surface wave poles;
4. It is as fast as CIM, and the memory requirement is also low;
5. It is easy to do error and accuracy control with LPFW.

Numerical results presented in this paper show the effectiveness and accuracy of the proposed method.

Acknowledgments

Wei Cai would like to thank the support of the National Science Foundation (grant number: DMS-0408309, CCF-0513179) and Department of Energy (grant Number: DEFG0205ER25678) for the work reported in this paper.

Appendix

I. Green's function in spectral domain (SD)

I.1 Green's function $\overline{\overline{\widetilde{G}}}_A$, $\widetilde{G}_V$

Let i be the source field layer index, j be the field layer index, however, they will be suppressed here. Let

$$\overline{\overline{\widetilde{G}}}_A = \begin{bmatrix} \widetilde{G}_A^{xx} & 0 & \widetilde{G}_A^{xz} \\ 0 & \widetilde{G}_A^{xx} & \widetilde{G}_A^{yz} \\ \widetilde{G}_A^{zx} & \widetilde{G}_A^{zy} & \widetilde{G}_A^{zz} \end{bmatrix}, \qquad \widetilde{G}_V = \frac{j}{\varepsilon_i}\widetilde{G}_{eyx}\frac{1}{4\pi}, \tag{A.1}$$

where

$$\widetilde{G}_A^{xx} = -j\mu_j\widetilde{G}_1\tfrac{1}{4\pi}, \qquad \widetilde{G}_A^{zx} = -jk_x\mu_j\widetilde{G}_{azx}\frac{1}{4\pi} \tag{A.2}$$

$$\widetilde{G}_A^{zy} = -jk_y\mu_j\widetilde{G}_{azx}\tfrac{1}{4\pi}, \qquad \widetilde{G}_A^{xz} = -jk_x\mu_j\widetilde{G}_{kxy}\frac{1}{4\pi} \tag{A.3}$$

$$\widetilde{G}_A^{yz} = -jk_y\mu_j\widetilde{G}_{kxy}\tfrac{1}{4\pi}, \qquad \widetilde{G}_A^{zz} = -j\mu_j\widetilde{G}_{hxz}\frac{1}{4\pi}. \tag{A.4}$$

In (A.1)-(A.4), when $i = j$

$$\begin{aligned}
\widetilde{G}_{eyx} &= -\frac{1}{k_{zi}}\left[\xi_0 - \frac{1}{k_\rho^2}k_{zi}^2(\widetilde{Q}_i^{Ve} - \widetilde{Q}_i^{Vh}) + \widetilde{Q}_i^{Vh}\right] = \widetilde{G}_{eyxQ} + \widetilde{G}_{eyxS}, \\
\nabla G_V &= \nabla G_{VQ} - (\cos\theta\hat{x} + \sin\theta\hat{y})\frac{j}{4\pi\varepsilon_i}S_1\left[\widetilde{G}_{eyxS}\right] + \hat{z}\frac{j}{4\pi\varepsilon_i}S_0[\widetilde{G}_{eyxzS}\Big], \\
\widetilde{G}_1 &= \frac{1}{k_{zi}}\left(\xi_0 + \widetilde{Q}_i^{Vh}\right) = \widetilde{G}_{1Q} + \widetilde{G}_{1S}, \\
\widetilde{G}_{hxz} &= \frac{1}{k_{zi}}\left[\xi_0 + \widetilde{Q}_i^{Ie} + \frac{k_{zi}^2}{k_\rho^2}\left(\widetilde{Q}_i^{Ih} - \widetilde{Q}_i^{Ie}\right)\right] = \widetilde{G}_{hxzQ} + \widetilde{G}_{hxzS}, \\
\widetilde{G}_{azx} &= -\frac{1}{k_\rho^2}\left(\widetilde{q}_i^{Ve} - \widetilde{q}_i^{Vh}\right), \qquad \widetilde{G}_{kxy} = -\frac{1}{k_\rho^2}\left(\widetilde{q}_i^{Ie} - \widetilde{q}_i^{Ih}\right),
\end{aligned}$$

where

$$\begin{aligned}
&\widetilde{G}_{eyxQ} = -\frac{\xi_0}{k_{zi}}, \quad \widetilde{G}_{1Q} = \widetilde{G}_{hxzQ} = \frac{\xi_0}{k_{zi}}, \quad \widetilde{G}_{1S} = \frac{1}{k_{zi}}\widetilde{Q}_i^{Vh}, \\
&\widetilde{G}_{eyxS} = \frac{1}{k_{zi}}\left[\frac{k_{zi}^2}{k_\rho^2}\left(\widetilde{Q}_i^{Ve} - \widetilde{Q}_i^{Vh}\right) - \widetilde{Q}_i^{Vh}\right], \\
&\widetilde{G}_{eyxzS} = -j\left[\frac{k_{zi}^2}{k_\rho^2}\left(\widetilde{q}_i^{Ve} - \widetilde{q}_i^{Vh}\right) - \widetilde{q}_i^{Vh}\right], \\
&\widetilde{G}_{hxzS} = \frac{1}{k_{zi}}\left[\widetilde{Q}_i^{Ie} + \frac{k_{zi}^2}{k_\rho^2}\left(\widetilde{Q}_i^{Ih} - \widetilde{Q}_i^{Ie}\right)\right].
\end{aligned}$$

In (A.1)-(A.4), when $j > i$

$$\widetilde{G}_{eyx} = \frac{1}{k_{zi}}\left[\xi_1 \widetilde{S}^V_{nji} + \frac{k^2_{zi}}{k^2_\rho}\widetilde{R}^{eh}_{nji} - \widetilde{Q}^{Vh}_i T^{Vh}_{nji}\right]$$

$$\widetilde{G}_{eyxz} = \frac{jk_{zj}}{k_{zi}}\left[\xi_1 \widetilde{s}^V_{nji} + \frac{k^2_{zi}}{k^2_\rho}\widetilde{r}^{eh}_{nji} - \widetilde{Q}^{Vh}_i T t^{Vh}_{nji}\right]$$

$$\widetilde{G}_1 = \frac{1}{k_{zi}}\left(\xi_1 + \widetilde{Q}^{Vh}_i\right) T^{Vh}_{nji}$$

$$\widetilde{G}_{hxz} = \frac{1}{k_{zi}}\left[C_n \xi_1 + A_n \widetilde{Q}^{Ie}_i + B_n \widetilde{Q}^{Ih}_i\right]$$

$$\widetilde{G}_{azx} = \frac{1}{k^2_\rho}\left[d_n \xi_1 + a_n \widetilde{Q}^{Ve}_i - b_n \widetilde{Q}^{Vh}_i\right]$$

$$\widetilde{G}_{kxy} = -\frac{1}{k^2_\rho}\frac{k_{zj}}{k_{zi}}\frac{\varepsilon_{ri}}{\varepsilon_{rj}}\left[\xi_1 N_1 + N_2 + N_3\right];$$

and when $j < i$

$$\widetilde{G}_{eyx} = \frac{1}{k_{zi}}\left[\xi_{-1} \widetilde{S}^V_{uji} + \frac{k^2_{zi}}{k^2_\rho}\widetilde{R}^{eh}_{uji} - \widetilde{Q}^{Vh}_i T^{Vh}_{uji}\right]$$

$$\widetilde{G}_{eyxz} = -\frac{jk_{zj}}{k_{zi}}\left[\xi_{-1} \widetilde{s}^V_{uji} + \frac{k^2_{zi}}{k^2_\rho}\widetilde{r}^{eh}_{uji} - \widetilde{Q}^{Vh}_i T t^{Vh}_{uji}\right]$$

$$\widetilde{G}_1 = \frac{1}{k_{zi}}\left(\xi_{-1} + \widetilde{Q}^{Vh}_i\right) T^{Vh}_{uji}$$

$$\widetilde{G}_{hxz} = \frac{1}{k_{zi}}\left[C_u \xi_{-1} + A_u \widetilde{Q}^{Ie}_i + B_u \widetilde{Q}^{Ih}_i\right]$$

$$\widetilde{G}_{azx} = -\frac{1}{k^2_\rho}\left[d_u \xi_{-1} + a_u \widetilde{Q}^{Ve}_i - b_u \widetilde{Q}^{Vh}_i\right]$$

$$\widetilde{G}_{kxy} = \frac{1}{k^2_\rho}\frac{k_{zj}}{k_{zi}}\frac{\varepsilon_{ri}}{\varepsilon_{rj}}\left[\xi_{-1} U_1 + U_2 + U_3\right].$$

where $\xi_0 = e^{-jk_{zi}|z-z'|}$, $\quad \xi_1 = e^{-jk_{zi}|z_i - z'|}$, $\quad \xi_{-1} = e^{-jk_{zi}|z_{i-1} - z'|}$

$$a_u = \tfrac{k_{zi}}{k_{zj}}\tfrac{\varepsilon_{rj}}{\varepsilon_{ri}}\left(T^{Ve}_{uji} + t^{Ve}_{uji}\right), \qquad b_u = \frac{k_{zj}}{k_{zi}}\frac{\mu_i}{\mu_j}\left(T^{Vh}_{uji} + t^{Vh}_{uji}\right),$$

$$a_n = \tfrac{k_{zi}}{k_{zj}}\tfrac{\varepsilon_{rj}}{\varepsilon_{ri}}\left(T^{Ve}_{nji} + t^{Ve}_{nji}\right), \qquad b_n = \frac{k_{zj}}{k_{zi}}\frac{\mu_i}{\mu_j}\left(T^{Vh}_{nji} + t^{Vh}_{nji}\right),$$

$$A_u = T^{Ie}_{uji}\left(1 - \tfrac{k^2_{zj}}{k^2_\rho}\tfrac{\varepsilon_{ri}\mu_i}{\varepsilon_{rj}\mu_j}\right), \qquad B_u = T^{Ih}_{uji}\left(\frac{k^2_{zi}}{k^2_\rho}\right),$$

$$A_n = T^{Ie}_{nji}\left(1 - \tfrac{k^2_{zj}}{k^2_\rho}\tfrac{\varepsilon_{ri}\mu_i}{\varepsilon_{rj}\mu_j}\right), \qquad B_n = T^{Ih}_{nji}\left(\frac{k^2_{zi}}{k^2_\rho}\right),$$

$$C_n = A_n + B_n, \qquad C_u = A_u + B_u,$$

$$d_n = a_n - b_n, \qquad d_u = a_u - b_u,$$

$$\widetilde{S}^V_{nji} = \frac{k^2_{zi}}{k^2_\rho}\left(T^{Ve}_{nji} - T^{Vh}_{nji}\right) - T^{Vh}_{nji}, \qquad \widetilde{S}^V_{uji} = \frac{k^2_{zi}}{k^2_\rho}\left(T^{Ve}_{uji} - T^{Vh}_{uji}\right) - T^{Vh}_{uji},$$

$$\widetilde{s}^V_{nji} = \frac{k^2_{zi}}{k^2_\rho}\left(Tt^{Ve}_{nji} - Tt^{Vh}_{nji}\right) - Tt^{Vh}_{nji}, \qquad \widetilde{s}^V_{uji} = \frac{k^2_{zi}}{k^2_\rho}\left(Tt^{Ve}_{uji} - Tt^{Vh}_{uji}\right) - Tt^{Vh}_{uji},$$

$$\widetilde{R}^{eh}_{nji} = \widetilde{Q}^{Ve}_i T^{Ve}_{nji} - \widetilde{Q}^{Vh}_i T^{Vh}_{nji}, \qquad \widetilde{R}^{eh}_{uji} = \widetilde{Q}^{Ve}_i T^{Ve}_{uji} - \widetilde{Q}^{Vh}_i T^{Vh}_{uji},$$

$$\widetilde{r}^{eh}_{nji} = \widetilde{Q}^{Ve}_i Tt^{Ve}_{nji} - \widetilde{Q}^{Vh}_i Tt^{Vh}_{nji}, \qquad \widetilde{r}^{eh}_{uji} = \widetilde{Q}^{Ve}_i Tt^{Ve}_{uji} - \widetilde{Q}^{Vh}_i Tt^{Vh}_{uji},$$

$$\chi^V_{nji} = k^2_{zi}\widetilde{Q}^{Ve}_i T^{Ve}_{nji} + k^2_i \widetilde{Q}^{Vh}_i \left(2\tfrac{\mu_j}{\mu_i} - 1\right) T^{Vh}_{nji}, \qquad \chi^V_{uji} = k^2_{zi}\widetilde{Q}^{Ve}_i T^{Ve}_{uji} + k^2_i \widetilde{Q}^{Vh}_i \left(2\frac{\mu_j}{\mu_i} - 1\right) T^{Vh}_{uji},$$

$$\mu_{ij} = \frac{k^2_{zi}}{k^2_\rho}\left(1 - \frac{\mu_j}{\mu_i}\right),$$

$$U_1 = Tt^{Ih}_{uji}\frac{k^2_{zi}}{k^2_{zj}}\frac{\varepsilon_{rj}\mu_j}{\varepsilon_{ri}\mu_i} - Tt^{Ie}_{uji}, \qquad N_1 = Tt^{Ih}_{nji}\frac{k^2_{zi}}{k^2_{zj}}\frac{\varepsilon_{rj}\mu_j}{\varepsilon_{ri}\mu_i} - Tt^{Ie}_{nji},$$

$$U_2 = \widetilde{Q}^{Ih}_i Tt^{Ih}_{uji}\frac{k^2_{zi}}{k^2_{zj}}\frac{\varepsilon_{rj}\mu_j}{\varepsilon_{ri}\mu_i}, \qquad N_2 = \widetilde{Q}^{Ih}_i Tt^{Ih}_{nji}\frac{k^2_{zi}}{k^2_{zj}}\frac{\varepsilon_{rj}\mu_j}{\varepsilon_{ri}\mu_i},$$

$$U_3 = -\widetilde{Q}^{Ie}_i Tt^{Ie}_{uji}, \qquad N_3 = -\widetilde{Q}^{Ie}_i Tt^{Ie}_{nji},$$

$$Tt^{Ih(e)}_{uji} = T^{Ih(e)}_{uji} + t^{Ih(e)}_{uji}, \qquad Tt^{Ih(e)}_{nji} = T^{Ih(e)}_{nji} + t^{Ih(e)}_{nji},$$

$$Tt^{Vh(e)}_{uji} = T^{Vh(e)}_{uji} + t^{Vh(e)}_{uji}, \qquad Tt^{vh(e)}_{nji} = T^{vh(e)}_{nji} + t^{Vh(e)}_{nji}.$$

In above formulas, $T, t, \widetilde{Q}, \widetilde{q}$ are defined as: when $j = i-1$:

$$T^{BC}_{ui-1,i} = \frac{e^{-jk_{zi-1}[z-z_{i-1}]}}{1 \pm R^C_{ui-1}e^{-j2\phi_{i-1}}}\left[1 \pm R^C_{ui-1}e^{-j2k_{zi-1}(z_{i-2}-z)}\right],$$

$$t^{BC}_{ui-1,i} = -\frac{e^{-j\phi_{i-1}}e^{-jk_{zi-1}[z-z_{i-2}]}}{1 \pm R^C_{ui-1}e^{-j2\phi_{i-1}}}\left[\pm 2R^C_{ui-1}e^{-j2k_{zi-1}(z_{i-2}-z)}\right];$$

when $j < i-1$:

$$T^{BC}_{uji} = \frac{e^{-jk_{zj}[z-z_j]}}{1 \pm R^C_{uj}e^{-j2\phi_j}}\left[1 \pm R^C_{uj}e^{-j2k_{zj}(z_{j-1}-z)}\right]\prod_{p=j}^{i-2}\frac{(1 \pm R^C_{up+1})e^{-j\phi_{p+1}}}{1 \pm R^C_{up+1}e^{-j2\phi_{p+1}}},$$

$$t^{BC}_{uji} = -\frac{e^{-jk_{zj}[z-z_j]}}{1 \pm R^C_{uj}e^{-j2\phi_j}}\left[\pm 2R^C_{uj}e^{-j2k_{zj}(z_{j-1}-z)}\right]\prod_{p=j}^{i-2}\frac{(1 \pm R^C_{up+1})e^{-j\phi_{p+1}}}{1 \pm R^C_{up+1}e^{-j2\phi_{p+1}}};$$

when $j = i+1$:

$$T^{BC}_{ni+1,i} = \frac{e^{-jk_{zi+1}[z_i-z]}}{1 \pm R^C_{ni+1}e^{-j2\phi_{i+1}}}\left[1 \pm R^C_{ni+1}e^{-j2k_{zi+1}(z-z_{i+1})}\right],$$

$$t^{BC}_{ni+1,i} = -\frac{e^{-j\phi_{i+1}}e^{jk_{zi+1}[z-z_{i+1}]}}{1 \pm R^C_{ni+1}e^{-j2\phi_{i+1}}}\left[\pm 2R^C_{ni+1}e^{-j2k_{zi+1}(z-z_{i+1})}\right];$$

and when $j > i+1$:

$$T^{BC}_{nji} = \frac{e^{-jk_{zj}(z_{j-1}-z)}}{1 \pm R^C_{nj} e^{-j2\phi_j}} \left[1 \pm R^C_{nj} e^{-j2k_{zj}(z-z_j)}\right] \prod_{p=i+1}^{j-1} \frac{(1 \pm R^C_{np}) e^{-j\phi_p}}{1 \pm R^C_{np} e^{-j2\phi_p}},$$

$$t^{BC}_{nji} = -\frac{e^{-jk_{zj}(z_{j-1}-z)}}{1 \pm R^C_{nj} e^{-j2\phi_j}} \left[\pm 2R^C_{nj} e^{-j2k_{zj}(z-z_j)}\right] \prod_{p=i+1}^{j-1} \frac{(1 \pm R^C_{np}) e^{-j\phi_p}}{1 \pm R^C_{np} e^{-j2\phi_p}};$$

for term T^{BC}_{Aji} $(A = u, n;\ B = V, I;\ C = e, h)$, if $B = V$, take "+" before R; if $B = I$, take "−" before R. Moreover,

$$\widetilde{Q}^{BC}_i(z, z') = \frac{1}{D^C_i}(\pm R^C_{ni} e_1 \pm R^C_{ui} e_2 + 2R^C_{ui} R^C_{ni} e_3),$$

$$\widetilde{q}^{BC}_i(z, z') = \frac{1}{D^C_i}(\pm R^C_{ni} e_1 - (\pm R^C_{ui}) e_2 - 2jR^C_{ui} R^C_{ni} e_4);$$

also for term $\widetilde{Q}^{BC}_i$, $\widetilde{q}^{BC}_i$, $(B = V, I;\ C = e, h)$, if $B = V$, take "+" before R; if $B = I$, take "−" before R, and

$$\begin{aligned}
&\text{for } i = j: \quad \widetilde{Q}^{BC}_i = \widetilde{Q}^{BC}_i(z, z'), \quad \widetilde{q}^{BC}_i = \widetilde{q}^{BC}_i(z, z'),\\
&\text{for } i > j: \quad \widetilde{Q}^{BC}_i = \widetilde{Q}^{BC}_i(z_{i-1}, z'), \quad \widetilde{q}^{BC}_i = \widetilde{q}^{BC}_i(z_{i-1}, z'),\\
&\text{for } i < j: \quad \widetilde{Q}^{BC}_i = \widetilde{Q}^{BC}_i(z_i, z'), \quad \widetilde{q}^{BC}_i = \widetilde{q}^{BC}_i(z_i, z');
\end{aligned}$$

for the ith layer, its top and bottom defined by z_{i-1} and z_i respectively, where

$$\begin{aligned}
&e_1 = e^{-jk_{zi}[(z+z')-2z_i]}, \quad e_2 = e^{-jk_{zi}[2z_{i-1}-(z+z')]},\\
&e_3 = e^{-j2\phi_i} \cos[k_{zi}(z - z')],\\
&e_4 = e^{-j2\phi_i} \sin[k_{zi}(z - z')],\\
&D^C_i = 1 - R^C_{ni} R^C_{ui} e^{-j2\phi_i},\\
&R^C_{ni} = \frac{Z^C_{ni} - Z^C_i}{Z^C_{ni} + Z^C_i},\\
&R^C_{ui} = \frac{Z^C_{ui} - Z^C_i}{Z^C_{ui} + Z^C_i},\\
&Z^C_{nk} = Z^C_{k+1} \frac{Z^C_{nk+1} + jZ^C_{k+1} t_{k+1}}{Z^C_{k+1} + jZ^C_{nk+1} t_{k+1}}, \quad k = i, i+1, \cdots,\\
&Z^C_{uk} = Z^C_{k-1} \frac{Z^C_{uk-1} + jZ^C_{k-1} t_{k-1}}{Z^C_{k-1} + jZ^C_{uk-1} t_{k-1}}, \quad k = i, i-1, \cdots 1,\\
&Z^h_k = Z^{TE}_k = \frac{\omega\mu_k}{k_{zk}}, \quad k = 0, 1, \cdots,\\
&Z^e_k = Z^{TM}_k = \frac{k_{zk}}{\omega\varepsilon_k}, \quad k = 0, 1, \cdots,\\
&t_k = \tan\phi_k, \quad \phi_k = k_{zk} h_k, \quad k = 0, 1, \cdots.
\end{aligned}$$

The relevant boundary conditions are given by:

- if the top space is open, $Z^C_{u0} = Z^C_0$, $R^C_{u0} = 0$;
- if the top space is closed by PEC, $Z^C_{u0} = 0$, $R^C_{u0} = -1$;
- if the bottom space is open, $Z^C_{nN} = Z^C_{N+1}$, $R^C_{nN+1} = 0$;
- if the bottom space is closed by PEC, $Z^C_{nN} = 0$, $R^C_{nN+1} = -1$.

I.2 Green's function $\overline{\overline{G}}_E$

From $\overline{\overline{G}}_E = -j\omega\overline{\overline{G}}_A - \frac{1}{j\omega}\nabla\nabla' G_V$ we have

$$\overline{\overline{G}}_E = \begin{bmatrix} \widetilde{G}^{xx}_E & \widetilde{G}^{xy}_E & \widetilde{G}^{xz}_E \\ \widetilde{G}^{yx}_E & \widetilde{G}^{yy}_E & \widetilde{G}^{yz}_E \\ \widetilde{G}^{zx}_E & \widetilde{G}^{zy}_E & \widetilde{G}^{zz}_E \end{bmatrix} \tag{A.5}$$

where

$$\widetilde{G}^{xx}_E = \left[(-jk_x)^2\widetilde{G}_{exx1} - (-jk_y)^2\widetilde{G}_{exx2}\right]\frac{1}{4\pi}, \tag{A.6}$$

$$\widetilde{G}^{yy}_E = \left[(-jk_y)^2\widetilde{G}_{exx1} - (-jk_x)^2\widetilde{G}_{exx2}\right]\frac{1}{4\pi}, \tag{A.7}$$

$$\widetilde{G}^{zz}_E = \widetilde{G}_5\frac{1}{4\pi}, \tag{A.8}$$

$$\widetilde{G}^{xy}_E = \widetilde{G}^{yx}_E = (-jk_x)(-jk_y)\widetilde{G}_{eyxw}\frac{1}{4\pi}, \tag{A.9}$$

$$\widetilde{G}^{zx}_E = -jk_x\widetilde{G}_3\frac{1}{4\pi}, \tag{A.10}$$

$$\widetilde{G}^{zy}_E = -jk_y\widetilde{G}_3\frac{1}{4\pi}, \tag{A.11}$$

$$\widetilde{G}^{xz}_E = -jk_x\widetilde{G}_{exz}\frac{1}{4\pi}, \tag{A.12}$$

$$\widetilde{G}^{yz}_E = -jk_y\widetilde{G}_{exz}\frac{1}{4\pi}; \tag{A.13}$$

and we redefine

$$\widetilde{G}_{exxm} = k_\rho^2(\widetilde{G}_{exx2} - \widetilde{G}_{exx1}) \tag{A.14}$$

$$\widetilde{G}_{eyxw} = (\widetilde{G}_{exx2} + \widetilde{G}_{exx1}) = \widetilde{G}_{eyx}/(\omega\varepsilon_i). \tag{A.15}$$

In the above formulas, when $i = j$:

$$\begin{aligned} G^{xx}_E &= \frac{1}{8\pi}\cos 2\theta S_2[\widetilde{G}_{eyxwS}] + \frac{1}{8\pi}S_0[\widetilde{G}_{exxmS}] - j\omega G^{xx}_{AQ} - \frac{1}{j\omega}\frac{\partial^2}{\partial x\partial x'}G_{VQ}, \\ G^{yy}_E &= -\frac{1}{8\pi}\cos 2\theta S_2[\widetilde{G}_{eyxwS}] + \frac{1}{8\pi}S_0[\widetilde{G}_{exxmS}] - j\omega G^{xx}_{AQ} - \frac{1}{j\omega}\frac{\partial^2}{\partial y\partial y'}G_{VQ}, \\ G^{zz}_E &= G^{zz}_{EQ} + \frac{1}{4\pi}S_0[\widetilde{G}_{5S}], \end{aligned}$$

$$
\begin{aligned}
G_E^{xy} &= G_E^{yx} = \frac{1}{8\pi}\cos 2\theta S_2[\widetilde{G}_{eyxwS}] + \frac{1}{j\omega}\frac{\partial^2}{\partial x\partial y}G_{VQ},\\
G_E^{xz} &= -\frac{1}{4\pi}\cos\theta S_1[\widetilde{G}_{exzS}] - \frac{1}{j\omega}\frac{\partial^2}{\partial x\partial z'}G_{VQ},\\
G_E^{yz} &= -\frac{1}{4\pi}\sin\theta S_1[\widetilde{G}_{exzS}] - \frac{1}{j\omega}\frac{\partial^2}{\partial y\partial z'}G_{VQ},\\
G_E^{zx} &= -\frac{1}{4\pi}\cos\theta S_1[\widetilde{G}_{3S}] + \frac{1}{j\omega}\frac{\partial^2}{\partial x\partial z}G_{VQ},\\
G_E^{zy} &= -\frac{1}{4\pi}\sin\theta S_1[\widetilde{G}_{3S}] + \frac{1}{j\omega}\frac{\partial^2}{\partial y\partial z}G_{VQ},\\
G_{VQ} &= \frac{1}{4\pi\varepsilon_i}\frac{e^{-jk_ir}}{r},\\
G_{AQ}^{xx} &= G_{AQ}^{yy} = G_{AQ}^{zz} = \frac{\mu_i}{4\pi}\frac{e^{-jk_ir}}{r};
\end{aligned}
$$

where $r = |r - r'|$ and

$$
\begin{aligned}
\widetilde{G}_{eyxwS} &= \frac{1}{\omega\varepsilon_i k_{zi}}\left[\frac{k_{zi}^2}{k_\rho^2}\left(\widetilde{Q}_i^{Ve} - \widetilde{Q}_i^{Vh}\right) - \widetilde{Q}_i^{Vh}\right],\\
\widetilde{G}_{exxmS} &= -\frac{1}{\omega\varepsilon_i k_{zi}}\left[k_{zi}^2\widetilde{Q}_i^{Ve} + k_i^2\widetilde{Q}_i^{Vh}\right],\\
\widetilde{G}_{5S} &= -\frac{k_\rho^2}{\omega\varepsilon_i k_{zi}}\widetilde{Q}_i^{Ie}, \quad \widetilde{G}_{3S} = \frac{j}{\omega\varepsilon_i}\widetilde{q}_i^{Ve},\\
\widetilde{G}_{exzS} &= \frac{j}{\omega\varepsilon_i}\widetilde{q}_i^{Ie}.
\end{aligned}
$$

If it is the different layers problem, then there is no extraction operation for the "direct" terms. When $j > i$:

$$
\begin{aligned}
\widetilde{G}_{eyxw} &= \frac{1}{\omega\varepsilon_i}\widetilde{G}_{eyx},\\
\widetilde{G}_{exxm} &= -\frac{1}{\omega\varepsilon_i k_{zi}}\left[\xi_1\left(k_i^2\left(2\frac{\mu_j}{\mu_i} - 1\right)T_{nji}^{Vh} + k_{zi}^2 T_{nji}^{Ve}\right) + \chi_{nji}^V\right],\\
\widetilde{G}_5 &= -\frac{k_\rho^2}{\omega\varepsilon_j k_{zi}}\left(\xi_1 + \widetilde{Q}_i^{Ie}\right)T_{nji}^{Ie},\\
\widetilde{G}_{exz} &= -\frac{jk_{zj}}{\omega\varepsilon_j k_{zi}}\left(\xi_1 + \widetilde{Q}_i^{Ie}\right)Tt_{nji}^{Ie},\\
\widetilde{G}_3 &= -\frac{jk_{zi}}{\omega\varepsilon_i k_{zj}}\left(\xi_1 + \widetilde{Q}_i^{Ve}\right)Tt_{nji}^{Ve};
\end{aligned}
$$

and when $j < i$:

$$
\widetilde{G}_{eyxw} = \frac{1}{\omega\varepsilon_i}\widetilde{G}_{eyx},
$$

$$\begin{aligned}
\widetilde{G}_{exxm} &= -\frac{1}{\omega\varepsilon_i k_{zi}}\left[\xi_{-1}\left(k_i^2\left(2\frac{\mu_j}{\mu_i}-1\right)T_{uji}^{Vh}+k_{zi}^2 T_{uji}^{Ve}\right)+\chi_{uji}^{V}\right],\\
\widetilde{G}_5 &= -\frac{k_\rho^2}{\omega\varepsilon_j k_{zi}}\left(\xi_{-1}+\widetilde{Q}_i^{Ie}\right)T_{uji}^{Ie}\\
\widetilde{G}_{exz} &= \frac{jk_{zj}}{\omega\varepsilon_j k_{zi}}\left(\xi_{-1}+\widetilde{Q}_i^{Ie}\right)Tt_{uji}^{Ie}\\
\widetilde{G}_3 &= \frac{jk_{zi}}{\omega\varepsilon_i k_{zj}}\left(\xi_{-1}+\widetilde{Q}_i^{Ve}\right)Tt_{uji}^{Ve}
\end{aligned}$$

I.3 Green's function $\overline{\overline{G}}_H$

From $\overline{G}_H=\frac{1}{\mu}\nabla\times\overline{G}_A$ one arrived

$$\overline{\overline{G}}_H=\begin{bmatrix}\widetilde{G}_H^{xx} & \widetilde{G}_H^{xy} & \widetilde{G}_H^{xz}\\ \widetilde{G}_H^{yx} & \widetilde{G}_H^{yy} & \widetilde{G}_H^{yz}\\ \widetilde{G}_H^{zx} & \widetilde{G}_H^{zy} & 0\end{bmatrix} \tag{A.16}$$

where

$$\widetilde{G}_H^{xx} = (-jk_x)(-jk_y)\widetilde{G}_{azx}\frac{1}{4\pi}, \tag{A.17}$$

$$\widetilde{G}_H^{yy} = -(-jk_x)(-jk_y)\widetilde{G}_{azx}\frac{1}{4\pi}, \tag{A.18}$$

$$\widetilde{G}_H^{xy} = \left[(-jk_y)^2\widetilde{G}_{azx}+j\widetilde{G}_1^z\right]\frac{1}{4\pi}, \tag{A.19}$$

$$\widetilde{G}_H^{yx} = -\left[(-jk_x)^2\widetilde{G}_{azx}+j\widetilde{G}_1^z\right]\frac{1}{4\pi}, \tag{A.20}$$

$$\widetilde{G}_H^{xz} = -(-jk_y)\left(\widetilde{G}_{kxy}^z+j\widetilde{G}_{hxz}\right)\frac{1}{4\pi}, \tag{A.21}$$

$$\widetilde{G}_H^{yz} = -jk_x\left(\widetilde{G}_{kxy}^z+j\widetilde{G}_{hxz}\right)\frac{1}{4\pi}, \tag{A.22}$$

$$\widetilde{G}_H^{zx} = -jk_y j\widetilde{G}_1\frac{1}{4\pi}, \tag{A.23}$$

$$\widetilde{G}_H^{zy} = -(-jk_x)j\widetilde{G}_1\frac{1}{4\pi}. \tag{A.24}$$

We redefine the following terms:

$$\widetilde{G}_1^z=\frac{\partial\widetilde{G}_1}{\partial z},\quad \widetilde{G}_h=\widetilde{G}_{kxy}^z+j\widetilde{G}_{hxz}, \tag{A.25}$$

$$\widetilde{G}_{kxy}^z=\frac{\partial\widetilde{G}_{kxy}}{\partial z},\quad \widetilde{G}_{azx\rho}=k_\rho^2\widetilde{G}_{azx}. \tag{A.26}$$

When $i=j$:

$$
\begin{aligned}
&G_H^{xx} = -G_H^{yy} = \frac{1}{8\pi}\sin 2\theta S_2[\widetilde{G}_{azx}], \quad G_H^{zz} = 0,\\
&G_H^{xy} = \frac{1}{\mu_i}\frac{\partial}{\partial z}G_{AQ}^{xx} - \frac{1}{8\pi}\cos 2\theta S_2[\widetilde{G}_{azx}] + \frac{1}{8\pi}S_0[\widetilde{G}_{hxyS}],\\
&G_H^{yx} = -\frac{1}{\mu_i}\frac{\partial}{\partial z}G_{AQ}^{xx} - \frac{1}{8\pi}\cos 2\theta S_2[\widetilde{G}_{azx}] - \frac{1}{8\pi}S_0[\widetilde{G}_{hxyS}],\\
&G_H^{xz} = -\frac{1}{\mu_i}\frac{\partial}{\partial y}G_{AQ}^{zz} + \frac{1}{4\pi}\sin\theta S_1[\widetilde{G}_{hS}],\\
&G_H^{yz} = \frac{1}{\mu_i}\frac{\partial}{\partial x}G_{AQ}^{zz} - \frac{1}{4\pi}\cos\theta S_1[\widetilde{G}_{hS}],\\
&G_H^{zx} = -\frac{1}{\mu_i}\frac{\partial}{\partial y}G_{AQ}^{xx} - \frac{j}{4\pi}\sin\theta S_1[\widetilde{G}_{1S}],\\
&G_H^{zy} = \frac{1}{\mu_i}\frac{\partial}{\partial x}G_{AQ}^{yy} + \frac{j}{4\pi}\cos\theta S_1[\widetilde{G}_{1S}],\\
&\widetilde{G}_{hxyS} = \widetilde{q}_i^{Ve} + \widetilde{q}_i^{Vh},\\
&\widetilde{G}_{hS} = \frac{j}{k_{zi}}\widetilde{Q}_i^{Ie},\\
&\widetilde{G}_{1S} = \frac{1}{k_{zi}}\widetilde{Q}_i^{Vh}.
\end{aligned}
$$

If it is the different layers problem, then there is no extraction operation for the "direct" terms. When $j>i$:

$$
\begin{aligned}
\widetilde{G}_h &= \frac{j}{k_{zi}}\left[\xi_1\left(T_{nji}^{Ie}+\mu_{ij}T_{nji}^{Ih}\right)+T_{nji}^{Ie}\widetilde{Q}_i^{Ie}+\mu_{ij}T_{nji}^{Ih}\widetilde{Q}_i^{Ih}\right],\\
\widetilde{G}_{hxy} &= 2j\widetilde{G}_{1z}-\widetilde{G}_{azx\rho}\\
&= -\xi_1\left(2Tt_{nji}^{Vh}\frac{k_{zj}}{k_{zi}}+d_n\right)-\widetilde{Q}_i^{Vh}\left(2Tt_{nji}^{Vh}\frac{k_{zj}}{k_{zi}}-b_n\right)-a_n\widetilde{Q}_i^{Ve};
\end{aligned}
$$

and when $j<i$:

$$
\begin{aligned}
\widetilde{G}_h &= \frac{j}{k_{zi}}\left[\xi_{-1}\left(T_{uji}^{Ie}+\mu_{ij}T_{uji}^{Ih}\right)+T_{uji}^{Ie}\widetilde{Q}_i^{Ie}+\mu_{ij}T_{uji}^{Ih}\widetilde{Q}_i^{Ih}\right],\\
\widetilde{G}_{hxy} &= 2j\widetilde{G}_{1z}-\widetilde{G}_{azx\rho}\\
&= \xi_{-1}\left(2Tt_{uji}^{Vh}\frac{k_{zj}}{k_{zi}}+d_u\right)+\widetilde{Q}_i^{Vh}\left(2Tt_{uji}^{Vh}\frac{k_{zj}}{k_{zi}}-b_u\right)+a_u\widetilde{Q}_i^{Ve}.
\end{aligned}
$$

I.4 The Spectral of ∇G_V

As in [13], we need $\nabla G_V = \hat{\rho}G_{Vxy} + \hat{z}G_{Vz}$ so, here we also define the following term:

$$\widetilde{G}_{eyxz} = \widetilde{G}_{eyx}^{z} = \frac{\partial \widetilde{G}_{eyx}}{\partial z}$$

where $\widetilde{G}_{eyx}$ has been defined in above subsections.

II. Green's function in spatial domain

II.1 Green's Function $\overline{G}_H(r/r')$

The components of the Green's Function $\overline{G}_H(r/r')$ are given by

$$G_H^{xx} = -G_H^{yy} = \frac{1}{8\pi}\sin 2\theta\ g_{hxx} \tag{A.27}$$

$$G_H^{zz} = 0 \tag{A.28}$$

$$G_H^{xy} = -\frac{1}{8\pi}(\cos 2\theta\ g_{hxx} + g_{h\rho}) + \frac{j}{4\pi}g_{h1z} \tag{A.29}$$

$$G_H^{yx} = -\frac{1}{8\pi}(\cos 2\theta\ g_{hxx} - g_{h\rho}) - \frac{j}{4\pi}g_{h1z} \tag{A.30}$$

$$G_H^{xz} = \frac{1}{4\pi}\sin\theta\ g_{h\rho z} \tag{A.31}$$

$$G_H^{yz} = -\frac{1}{4\pi}\cos\theta\ g_{h\rho z} \tag{A.32}$$

$$G_H^{zx} = -j\frac{1}{4\pi}\sin\theta\ g_{hz\rho} \tag{A.33}$$

$$G_H^{zy} = j\frac{1}{4\pi}\cos\theta\ g_{hz\rho} \tag{A.34}$$

where $\theta = \arcsin(x - x')/\rho$.

II.2 Green's Function $\overline{G}_E(r/r')$

The components of the Green's Function $\overline{G}_E(r/r')$ are given by

$$G_E^{xx} = \frac{1}{8\pi}\cos 2\theta\ g_{exx1} + \frac{1}{8\pi}g_{exx2} \tag{A.35}$$

$$G_E^{yy} = -\frac{1}{8\pi}\cos 2\theta\ g_{exx1} + \frac{1}{8\pi}g_{exx2} \tag{A.36}$$

$$G_E^{zz} = \frac{1}{4\pi}\ g_{ezz} \tag{A.37}$$

$$G_E^{xy} = G_E^{yx} = \frac{1}{8\pi}\sin 2\theta\ g_{exx1} \tag{A.38}$$

$$G_E^{xz} = -\frac{1}{4\pi}\cos\theta\ g_{e\rho z} \tag{A.39}$$

$$G_E^{yz} = -\frac{1}{4\pi}\sin\theta\ g_{e\rho z} \tag{A.40}$$

$$G_E^{zx} = -\frac{1}{4\pi}\cos\theta\ g_{ez\rho} \tag{A.41}$$

$$G_E^{zy} = -\frac{1}{4\pi}\sin\theta\ g_{ez\rho} \tag{A.42}$$

II.3 Green's Function $\overline{G}_A(r/r')$

The components of the Green's Function $\overline{G}_A(r/r')$ are given by

$$G_A^{xx} = G_A^{yy} = -\frac{\mu_j}{4\pi}\, g_{axx}, \tag{A.43}$$

$$G_A^{zz} = -\frac{\mu_j}{4\pi}\, g_{azz}, \tag{A.44}$$

$$G_A^{zx} = -\frac{\mu_j}{4\pi}\cos\theta\, g_{az\rho}, \tag{A.45}$$

$$G_A^{zy} = -\frac{\mu_j}{4\pi}\sin\theta\, g_{az\rho}, \tag{A.46}$$

$$G_A^{xz} = -\frac{\mu_i}{4\pi}\cos\theta\, g_{a\rho z}, \tag{A.47}$$

$$G_A^{yz} = -\frac{\mu_i}{4\pi}\sin\theta\, g_{a\rho z}. \tag{A.48}$$

II.4 Green's Function $G_V(r/r')$ and $\nabla G_V(r/r')$

The components of the Green's Function $G_V(r/r')$ and $\nabla G_V(r/r')$ are given by

$$G_V = \frac{j}{\varepsilon_i}\frac{1}{4\pi} g_v, \quad \nabla G_V = G_{V\rho}(\hat{x}\cos\theta + \hat{y}\sin\theta) + \hat{z} G_{Vz}, \tag{A.49}$$

$$G_{V\rho} = -\frac{j}{\varepsilon_i}\frac{1}{4\pi} g_{v\rho}, \quad G_{Vz} = \frac{j}{\varepsilon_i}\frac{1}{4\pi} g_{vz}. \tag{A.50}$$

III. Sommerfeld Transform

We define the Fourier Transform (FT) pair as below:

$$F\{f(x,y)\} = \widetilde{f}(k_x,k_y) = \frac{1}{2\pi}\int_{-\infty}^{\infty}\int_{-\infty}^{\infty} f(x,y) e^{j(k_x x + k_y y)} dx dy, \tag{A.51}$$

$$F^{-1}\{\widetilde{f}(k_x,k_y)\} = f(x,y) = \frac{1}{2\pi}\int_{-\infty}^{\infty}\int_{-\infty}^{\infty} \widetilde{f}(k_x,k_y) e^{-j(k_x x + k_y y)} dk_x dk_y. \tag{A.52}$$

Change x, y coordinates into polar coordinates in both the transform and space domain by:$x - x' = \rho\cos\theta, y - y' = \rho\sin\theta, k_x = k_\rho\cos\alpha, k_y = k_\rho\sin\alpha, k_\rho^2 = k_x^2 + k_y^2$, $\rho^2 = (x-x')^2 + (y-y')^2$, $\theta = \arctan((y-y')/(x-x'))$, $\alpha = \arctan(k_y/k_x)$ and also use the n^{th} order of *Bessel* function J_n:

$$J_n(z) = \frac{1}{2\pi}\int_0^{2\pi} \cos(n\theta - jz\sin\theta) d\theta. \tag{A.53}$$

The inverse Fourier integral can be conveniently expressed in terms of the Sommerfeld-type integrals of the form:

$$S_n\left[\widetilde{f}(k_\rho)\right] = \int_0^{\infty} \widetilde{f}(k_\rho) J_n(k_\rho\rho) k_\rho^{n+1} dk_\rho. \tag{A.54}$$

Take operation of $\partial/\partial x$, $\partial/\partial y$, $\partial^2/\partial x^2$, $\partial^2/\partial y^2$, at both sides of (A.52), we have the following relations:

$$F^{-1}\left\{\widetilde{f}(k_\rho)\right\} = S_0\left[\widetilde{f}(k_\rho)\right] \tag{A.55}$$

$$F^{-1}\left\{-jk_x\widetilde{f}(k_\rho)\right\} = -\cos\theta S_1\left[\widetilde{f}(k_\rho)\right] \tag{A.56}$$

$$F^{-1}\left\{-jk_y\widetilde{f}(k_\rho)\right\} = -\sin\theta S_1\left[\widetilde{f}(k_\rho)\right] \tag{A.57}$$

$$F^{-1}\left\{k_x^2\widetilde{f}(k_\rho)\right\} = -0.5\left\{\cos 2\theta S_2\left[\widetilde{f}(k_\rho)\right] - S_0\left[k_\rho^2\widetilde{f}(k_\rho)\right]\right\} \tag{A.58}$$

$$F^{-1}\left\{k_y^2\widetilde{f}(k_\rho)\right\} = 0.5\left\{\cos 2\theta S_2\left[\widetilde{f}(k_\rho)\right] + S_0\left[k_\rho^2\widetilde{f}(k_\rho)\right]\right\} \tag{A.59}$$

$$F^{-1}\left\{k_xk_y\widetilde{f}(k_\rho)\right\} = -0.5\sin 2\theta S_2\left[\widetilde{f}(k_\rho)\right]. \tag{A.60}$$

References

[1] Tiejun Yu and L. Carin, Electromagnetic-inductive response of a Dielectric void in a soil background, IEEE Trans. Geosci. Remote Sensing, 38(3) (2000).

[2] W. Shi, J. Liu, N. Kakani and Tiejun Yu, A fast hierarchical algorithm for 3-D capacitance extraction, in: Proc. 35th DAC, San Francisco, 1998, pp. 212-217.

[3] S. M. Rao, D. R. Wilton and A. W. Glisson, Electromagnetic scattering by surfaces of arbitrary shape, IEEE Trans. Antennas and Propagation, 30 (1982), 409-418.

[4] T. J. Cui and W. C. Chew, Fast evaluation of Sommerfeld integrals for EM wave scattering and radiation by three-dimensional buried objects, Technical Report, Electromagnetic Laboratory, University of Illinois at Urbana-Champaign, 1997.

[5] T. J. Cui and W. C. Chew, Efficient evaluation of Sommerfeld integrals for TM wave scattering by buried objects, J. Electromagnetic Wave Appl., 12 (1998), 607-657.

[6] K. Nabors and J. White, Fastcap: A multipole accelerated 3-D capacitance extraction program, IEEE Trans. Comput. Aid. Design of Integrated Circuits Syst., 10 (1991), 1447-1459.

[7] J. R. Phillips and J. White, A precorrected-FFT method for capacitance extraction of complicated 3-D structures, in: IEEE/ACM Int. Conf. on CAD, 1994, pp. 268-271.

[8] Tatsuo Itoh, Numerical Techniques for Microwave and Millimeter-wave Passive Structures, John Wiley & Sons, Inc., 1989.

[9] M. I. Aksun, A robust approach for the derivation of closed-form Green's functions, IEEE Trans, Micro. Theory Tech., 44 (1996), 651-658.

[10] Y. L. Chow, J. J. Yang, D. G. Fang and G. E. Howard, A closed-form spatial Green's functions for the thick microstrip substrate, IEEE Trans. Micro. Theory Tech., 39 (1991), 588-592.

[11] K. Michalski and D. Zheng, Electromagnetic scattering and radiation by surfaces of arbitrary shape in layered media, part I: Theory, IEEE Trans. Antennas and Propagation, 38 (1990), 335-344.

[12] K. Michalski and J. R. Mosig, Multilayered media Green's functions in the integral equation formulations, IEEE Trans. Antennas and Propagation, 45 (1997), 508-519.

[13] T. M. Habashy, R. W. Groom and B. Spies, Beyond the Born and Rytov approximations: A nonlinear approach to electromagnetic scattering, J. Geophys. Res., 98(B2) (1993), 1759-1775.

[14] L. Carin, N. Geng, M. McClure, J. Sichina and L. Nguyen, Ultra-wideband synthetic aperture radar for mine-field detection, IEEE Antennas Propagat. Mag., 41(1) (1993), 18-33.

[15] V. Rokhlin, Rapid solution of integral equation of scattering theory in two dimensions, J. Comput. Phys., 86 (1990), 414-439.
[16] C. H. Chan and R. A. Kipp, Application of the complex image method to multilevel, multiconductor microstrip lines, Int. J. Microwave Mill., 7 (1997), 359-367.
[17] A. Sommerfeld, Partial Differential Equations in Physics, New York: Academic Press, 1949, p. 242.
[18] Y. Hua and T. K. Sarkar, Generalized Pencil-of-Function Method for Extracting Poles of an EM System from Its Transient Response, IEEE Trans. Antennas and Propagation, 37 (1989), 229-2344.
[19] R. Coifman, V. Rokhlin and S. Wandzura, The fast multipole method for the wave equation: A pedestrian prescrition, IEEE Antennas Propagat. Mag., 35 (1993), 7-12.
[20] N. Geng , A. Sullivan and L. Carin, FMM for Scattering from an Arbitrary PEC Target above or Buried in a Lossy Half Space, IEEE Trans. Antennas and Propagation, 49(5) (2001), 740-748.
[21] J. M. Song and W. C. Chew, Fast multipole method solution using parameteric gentry, Microw. Opt. Techn. Let., 7 (1994), 760-765.
[22] J. M. Song, C. C. Lu and W. C. Chew, Multilevel fast multipole algorithm for electromagnetic scattering by large complex objects, IEEE Trans. Antennas and Propagation, 45 (1997), 1488-1493.
[23] E. Bleszynski, M. Bleszynski and T. Jaroszewicz, AIM: Adaptive integral method for solving large-scale electromagnetic scattering and radiation problems, Radio Science, 31 (1996), 1225-1251.
[24] J. R. Mosig, Integral Equation Technique in Numerical Techniques for Microwave and Millimeter-Wave Passive Structure, in: T. Itoh, (Ed.), New York, Wiley, 1989, pp. 133-213.
[25] R. F. Harrington, Field Computation by Moment Methods, New York: Macmillian, 1968.
[26] W. Cai and Tiejun Yu, High order mixed RWG basis functions for electromagnetic scattering and applications, IEEE Trans. Micro. Theory Tech., 49(7) (2001), 1295-1303.
[27] W. Cai and Tiejun Yu, Fast calculation of dyadic Green's function for electromagnetic scattering in the multi-layered medium, J. Comput. Phys., 165 (2000), 1-21.
[28] Tiejun Yu and W. Cai, High order window functions and fast algorithms for calculating dyadic Green's function in the multi-layered media, Radio Science, 36(4) (2001), 559-570.
[29] J. A. Stratton, Electromagnetic Theory , McGraw-Hill, New York, 1941.
[30] A. Erteza and B. K. Park, Non-uniqueness of resolution of Hertz vector in presence of a boundary, and the horizontal problem, IEEE Trans. Antennas and Propagation, 17 (1969), 376-378, 1969.
[31] K. A. Michalski, On the scalar potential of a point charge associated with a time-harmonic dipole in a layerd medium, IEEE Trans. Antennas and Propagation, 35(11) (1987), 1299-1301.
[32] A. Sommerfeld, Partial Differential Equations in Physics, Academic Press, New York, 1964.
[33] J. Van Bladel, Singular Electromagnetic Fields and Sources, IEEE Press, New York, 1991.